

**MACROCYCLE LIGAND MODIFICATIONS IN THE PURSUIT OF
NICKEL-OXYGEN COMPLEXES**

by

Joliene Trujillo

A thesis submitted to the Faculty of the University of Delaware in partial
fulfillment of the requirements for the degree of Master of Science in Chemistry

Spring 2010

Copyright 2010 Joliene Trujillo
All Rights Reserved

**MACROCYCLE LIGAND MODIFICATIONS IN THE PURSUIT OF
NICKEL-OXYGEN COMPLEXES**

by
Joliene Trujillo

Approved: _____
Charles G. Riordan, Ph.D.
Professor in charge of thesis on behalf of the Advisory Committee

Approved: _____
Klaus H. Theopold, Ph.D.
Chair of the Department of Chemistry and Biochemistry

Approved: _____
George H. Watson, Ph.D.
Interim Dean of the College of Arts and Sciences

Approved: _____
Debra Hess Norris, MS.
Vice Provost for Graduate and Professional Education

ACKNOWLEDGMENTS

I am very grateful to a number of people who have played an important role in my education. First, Charlie, I would like to thank you for support and guidance over the past four years. The excitement and enjoyment of chemistry you have exhibited will always be appreciated. I would also like to thank my committee members, Dr. Brian Bahnson, Dr. Svilen Bobev, and Dr. George Luther for their guidance and counsel.

A special thanks is owed to Andrea Jones, my high school chemistry teacher. Her love for science and devotion to education played a key role in my decision to pursue chemistry further. The summer prior to beginning my collage education, she tutored me and helped spark my love for science. I am deeply indebted to her. Special thanks are also due to Dr. David Pringle, University of Northern Colorado, who spent much time mentoring me while completing undergraduate research. I am thankful for all he has taught me and grateful for his patience and generosity. If not for these outstanding faculty members, and many others, I would not be here today.

My time at the University of Delaware has been very enjoyable. I am deeply indebted to a number of co-workers who I have had the privilege of working with: Nate Eckert, Matthew Kieber-Emmons, Micheal Mock, Piya Ariyananda, Megan Shalaida, Molly O'Hagan-Mock, Tina Tao, YingXin Huang, Bill Green, Mike Dao, Srimoyee Dasgupta, Jessica Wallick, and Peng Wang. My time here has also been blessed with a number of enjoyable friendships who have aided in my love and understanding of chemistry: Andrew DeAngelis, Chris Nelson, Laural Fisher, Gaby Uceda, Luke Ceo, Matthew Hassink, and Micheal Taylor. In my time here I have

learned how important it is to have an excellent staff and would like to thank the following for their support: Susan Cheadle (secretary), Jim Cleaver (instrument specialist), John Famiglietti (Sr. electronics specialist), Doug Nixon (master glass technologist), Steve Bai (NMR specialist), John Dykins (mass spectrometrists), Glenn Yap (X-ray crystallographer), Dr. Joe Fox (GC-MS), Dr. Colin Thorpe (CBI program) and Dr. John Koh (CBI program).

Lastly, to my amazing family who has supported me and encouraged me in every decision I made. My mother, Brenda, demonstrates a love for learning that inspires me to always continue to reach for a greater understanding of our world and the people in it. She is and always will be my hero. To my sister Crystal, who taught me what true strength of character is and my brother, Shawn, who has shown me perseverance and faith in all aspects of life. Of course, I cannot forget my niece and nephew, Kathryn and Gabriel, who have reminded me everyday to have fun and enjoy life, as only a child can do. To my grandparents, whom have both passed away, thank you for being my second set of parents, for encouraging me, protecting me, and always being a part of my life. I am thankful to have had the opportunity to continue my education and it would mean nothing if not for the support of my family. Through Him all things are possible.

TABLE OF CONTENTS

LIST OF TABLES	viii
LIST OF FIGURES	ix
ABSTRACT	xi
INTRODUCTION	1
1.1 Nickel and Oxygen in Biology	2
1.1.1 Aci-Reductone Dioxygenase	2
1.1.2 Superoxide Dismutase	4
1.2 Synthetic Mimics	6
1.2.1 Nickel-Oxygen Complexes Formed from H ₂ O ₂	7
1.2.2 Nickel-Oxygen Complexes Formed from Alternative Oxygen Atom Donors	9
1.2.3 Nickel-Oxygen Complexes Formed from Dioxygen	10
1.3 Summary	17
PHYSICAL METHODS AND LIGAND SYNTHESIS	19
2.1 Physical Methods	19
2.1.1 Nuclear Magnetic Resonance Spectroscopy	19
2.1.2 Infrared Spectroscopy	19
2.1.3 Mass Spectroscopy	20
2.1.4 Electronic Absorption Spectroscopy	20
2.1.5 Electron Paramagnetic Resonance Spectroscopy	21
2.1.6 X-Ray diffraction	21
2.1.7 Gas Chromatography	22

2.2 Experimental	22
2.2.1 Synthesis of Tetraneopentyl Cyclam	22
2.2.2 Metal-Based Oxidative Decomposition of TNPC	25
2.2.3 Synthesis of [Pd(TNPC)]Cl ₂	25
2.2.4 Synthesis of [Ni(tmcyclen)](OTf) ₂	26
2.3 Ligands.....	26
2.3.1 Tetraneopentyl Cyclam	27
2.3.1.1 Attempted Metalation of TNPC	27
2.3.1.2 Metal-Mediated Oxidative Decomposition of TNPC.....	30
2.3.2 The Tmcyclen Macrocyclic.....	32
2.3.2.1 Synthesis of [Ni(tmcyclen)]OTf and [Ni(tmcyclen)(CO)]OTf	33
2.4 Summary	34
SYNTHESIS AND REACTIVITY OF [Ni(TMCYCLEN)(O ₂)]OTf	36
3.1 Synthesis of [Ni(tmcyclen)(O ₂)]OTf.....	36
3.2 Activation of O ₂ by [Ni(tmcyclen)]OTf.....	40
3.3 Reactivity of [Ni(tmcyclen)(O ₂)]OTf	44
3.3.1 Reactivity Studies Protocol.....	44
3.3.2 Reaction of [Ni(tmcyclen)(O ₂)]OTf with Phosphines, Sulfides, Olefins, and Activated C-H Bonds	44
3.3.3 Reaction of [Ni(tmcyclen)(O ₂)]OTf with Substituted Phenols	45
3.3.4 Reactivity Studies when PhIO is used as an Oxygen Atom Donor	47

3.4 Oxygen Transfer by [Ni(tmcyclen)(O ₂)]OTf and [Ni(TMC)(O ₂)]OTf.....	49
3.5 Conclusions	52
REFERENCES	54
APPENDIX A: CRYSTALLOGRAPHIC DATA.....	60

LIST OF TABLES

Table 3.1	Products and yields for substituted phenol reactivity studies	47
Table 3.2	Products and yields for reactivity studies utilizing PhIO as an oxo-transfer agent.....	49

LIST OF FIGURES

Figure 1.1	Enzymatic reactions catalyzed by ARD	3
Figure 1.2	Proposed enzymatic mechanism for NiSOD.....	5
Figure 1.3	Nickel oxygen motifs A) bis(μ -oxo) B) bis(μ -superoxo) C) μ -oxo D) μ_6 -peroxo E) “side-on” peroxo or “side-on” superoxo F) “end- on” superoxo G) Trans-peroxo dimer.....	7
Figure 1.4	Formation of a bis(μ -oxo) complex leading to ligand oxidation	8
Figure 1.5	Epoxidation of an olefin by a nickel complex upon reaction with PhIO	10
Figure 1.6	Activation of dioxygen with a Ni^{2+} complex capable of oxidizing aromatic substrates. The major product was ligand oxidation ($\text{R} =$ H , F , CH_2CH_3 , $\text{CH}_2\text{C}_6\text{H}_5$	12
Figure 1.7	Activation of dioxygen by a $\text{Ni}(0)$ complex to form a monomeric “side-on” peroxo complex	13
Figure 1.8	Summary of the activation of dioxygen by $[\text{PhTt}^{\text{R}}]\text{Ni}(\text{CO})$	15
Figure 1.9	Summary of the activation of dioxygen by $[\text{Ni}(\text{TMC})]^+$	17
Figure 2.1	Structure of tetrapivaloyl cyclam as determined by X-ray diffraction. Thermal ellipsoids drawn at 30%. Hydrogen atoms not shown.	23
Figure 2.2	Structure of TNPC as determined by X-ray diffraction. Thermal ellipsoids drawn at 30%. Hydrogen atoms not shown.....	24
Figure 2.3	Mass Spectral data for $[\text{Pd}(\text{TNPC})]\text{Cl}_2$. A) Experimental ESI-MS spectrum with $m/z = 659.2$ ($\text{M}+\text{H})^+$ B) Theoretical Isotopic distribution pattern for $([\text{Pd}(\text{TNPC})]\text{Cl}_2+\text{H})^+$. --- Average mass - -- Monoisotopic Mass	30

Figure 2.4	Oxidative decomposition product of TNPC. Two macrocycles co-crystallized with CuCl_4^{2-} per unit cell. Thermal ellipsoids drawn at 30%. Hydrogen atoms not shown.	31
Figure 2.5	Oxidative decomposition product of TNPC, included for clarity	32
Figure 2.6	Crystal structure of $[\text{Ni}(\text{tmcyclen})(\text{CO})]\text{OTf}$. Thermal ellipsoids drawn at 30%. Hydrogen atoms and OTf anion not shown.	34
Figure 3.1	Electronic absorption spectrum of $[\text{Ni}(\text{tmcyclen})(\text{O}_2)](\text{OTf})$ in CH_3CN	37
Figure 3.2	Structure of $[\text{Ni}(\text{tmcyclen})(\text{O}_2)]^+$ as determined by Cho <i>et. al.</i>	39
Figure 3.3	Electronic absorption spectrum of $[\text{Ni}(\text{tmcyclen})\text{O}_2]^+$ formed via reaction of $[\text{Ni}(\text{tmcyclen})](\text{OTf})_2$ and KO_2 in DMSO.	40
Figure 3.4	Electronic absorption spectrum showing the decrease of the $[\text{Ni}(\text{tmcyclen})(\text{CO})]^+$ complex, giving rise to features assigned to the $[\text{Ni}(\text{tmcyclen})(\text{O}_2)]^+$. Scans taken every 60 seconds.	41
Figure 3.5	Electronic paramagnetic resonance spectrum of $[\text{Ni}(\text{tmcyclen})(\text{O}_2)]^+$ in THF, formed from reaction of $[\text{Ni}(\text{tmcyclen})(\text{CO})]^+$ with O_2 . Parameters - frequency: 9.355 GHz, microwave power: 1.002 mW, attenuation: 23 dB, receiver gain: 49 dB, modulation amplitude: 2 G, modulation frequency: 100 kHz, time constant and conversion time: 163.84 ms.	42
Figure 3.6	Electronic paramagnetic resonance spectrum of $[\text{Ni}(\text{tmcyclen})\text{O}_2]^+$ in THF at 4.2 K and the fit of that data by WEPR program.	43
Figure 3.7	Optical spectrum results for reaction of $[\text{Ni}(\text{tmcyclen})(\text{O}_2)](\text{OTf})$ with $(\text{PhTt}^{t\text{Bu}})\text{Ni}(\text{CO})$ in THF at -78°C . Features, $\lambda_{\text{max}} = 410$ and 565 nm, are in accord with formation of $[(\text{PhTt}^{t\text{Bu}})\text{Ni}]_2(\mu\text{-O})_2$	51
Figure 3.8	Optical spectrum results for reaction of $[\text{Ni}(\text{TMC})(\text{O}_2)](\text{OTf})$ with $(\text{PhTt}^{t\text{Bu}})\text{Ni}(\text{CO})$ in THF at -78°C . Features, $\lambda_{\text{max}} = 410$ and 565 nm, are in accord with formation of $[(\text{PhTt}^{t\text{Bu}})\text{Ni}]_2(\mu\text{-O})_2$	52

ABSTRACT

The utility of small molecules lies in the ability to alter the structure of the molecule and examine the spectroscopic characteristics as well as the reactivity of the complex. Small molecules are often used to probe mechanistic questions on much more complicated systems, such as enzymes. In 1996 a new form of superoxide dismutase was discovered which had nickel in the active site of the enzyme. This discovery sparked renewed interest in nickel-oxygen chemistry. Small molecules were used to probe different nickel-oxygen structure types and their spectroscopic characteristics, though complete understanding of the implications when altering the small molecules has yet to develop.

This thesis addresses macrocycle ligand modifications, the varying ways of synthesizing nickel-oxygen complexes, and the reactivity of the nickel-oxygen adducts with exogenous substrates. The work presented herein, describes the synthesis and characterization of $[\text{Ni}(\text{tmcyclen})(\text{CO})](\text{OTf})$. Subsequent oxygen activation by $[\text{Ni}(\text{tmcyclen})(\text{CO})](\text{OTf})$ lead to the formation of "side-on" nickel(III) peroxo complex as determined by electronic absorption spectroscopy, electron paramagnetic resonance spectroscopy, and mass spectroscopy. Alternatively, the complex can be synthesized from nickel(II) and reduced oxygen reagents, H_2O_2 or KO_2 . Reactivity studies of the $[\text{Ni}(\text{tmcyclen})(\text{O}_2)](\text{OTf})$ with phosphines, sulfides, olefins, activated C-

H bonds, and substituted phenols were investigated. The reactivity studies completed on the “side-on” nickel(III)-peroxo complex shed light on the electronic characteristics of the complex. This thesis represents the first time a “side-on” nickel(III)-peroxo complex is synthesized from monovalent nickel and dioxygen.

Chapter 1

INTRODUCTION

Approximately 2.4 billion years ago the Earth experienced a radical atmospheric transformation, going from a slightly reducing atmosphere to an oxidizing atmosphere. The Earth's early atmosphere consisted mostly of water vapor and carbon dioxide, with very little atmospheric oxygen. Photosynthetic organisms, such as cyanobacteria, utilized the carbon dioxide in the atmosphere as a carbon source, while exploiting water as an electron donor, forming oxygen as a byproduct. The oxygen began to accumulate giving rise to an oxidizing atmosphere allowing for the evolution of animal life.^[1, 2]

Organisms take advantage of readily available atmospheric oxygen for a number of cellular processes. The most well known proteins of which are the oxygen binding proteins, myoglobin and hemoglobin. These structurally related proteins exploit an iron porphyrin to reversibly bind and transport dioxygen.^[3] Another enzyme that utilizes dioxygen found in many different organisms is cytochrome P450. The most common enzymatic reaction catalyzed by P450 is a monooxygenase reaction, whereby one atom of the oxygen is inserted into the organic substrate while the other atom of oxygen is reduced to water. The transformation requires reductive activation of the dioxygen using reducing equivalents provided by NAD(P)H.^[4]

The active site for both classes of proteins contains an iron porphyrin complex. Dioxygen binding and activation by iron proteins has been extensively studied. However, iron is not the only metal found in biology to bind or activate dioxygen, For example, hemocyanin is a binuclear copper oxygen transport protein found in mulluscs and some arthropods.^[5] Dopamine β -monooxygenase and peptidylglycine α -hydroxylating monooxygenase are two copper containing proteins which activate dioxygen to convert dopamine to norepinephrine and C-terminal glycine-extended peptides to their α -hydroxylated products, respectively.^[6] Recently, the nickel containing enzymes aci-reductone dioxygenase (NiARD) and superoxide dismutase (NiSOD) have been shown to utilize dioxygen, or its reduced form superoxide, during catalysis.^[7, 8]

1.1 Nickel and Oxygen in Biology

1.1.1 Aci-Reductone Dioxygenase

Aci-reductone dioxygenase is a 20 kDa enzyme involved in the methionine salvage pathway. ARD plays a key role in maintaining the concentration of the substrate, S-methylthioadenosine, a metabolite derived from methionine known to be an inhibitor of polyamine biosynthesis and transmethylation reactions.^[9] ARD is unique in that it is capable of catalyzing two different reactions depending on the identity of the metal in the active site.^[9] In the iron form of the enzyme, 1,2-

dihydroxy-3-keto-5-methylthiopentane, is oxidized to the α -keto acid, which is then subsequently converted to methionine. The nickel form of the protein activates the same substrate converting it to methylthiopropionate, formate, and carbon monoxide, in what is considered the unproductive branch of the salvage pathway.^[9] The utility of the unproductive branch remains unknown, although it has been hypothesized that the carbon monoxide produced may play a role as a neurotransmitter (Figure 1.1).^[10]

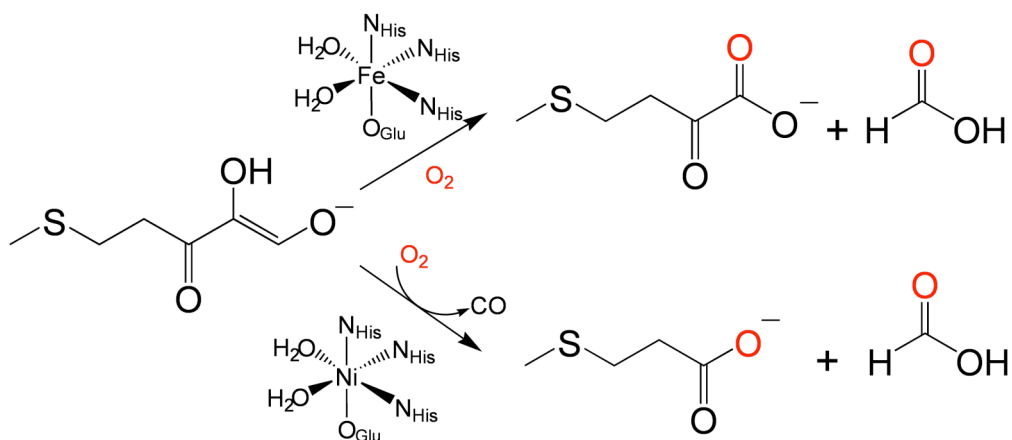


Figure 1.1 Enzymatic reactions catalyzed by ARD

The nickel site is octahedral and is coordinated by three histidine residues, one glutamic acid residue, and 2 unidentified labile ligands.^[11] NiARD was verified to act as a dioxygenase through labeling studies. Mechanistic studies also indicated that the nickel does not undergo redox changes but acts as a Lewis acid,

binding and activating the substrate towards dioxygen.^[12] Though the utility of NiARD is still not understood it is currently the only known nickel dioxygenase.

1.1.2 Superoxide Dismutase

Superoxide dimutases (SOD) are responsible for the disproportionation of superoxide, a cytotoxic reactive oxygen species, into hydrogen peroxide and dioxygen. There are four classes of SOD's, the Cu-Zn, Mn, Fe and the most recently discovered Ni. Nickel-containing superoxide dismutase was discovered in 1996 in the soil bacteria *Streptomyces coelicolor*.^[13] The enzyme has six identical 13.4 KDa subunits, each bound to one nickel at the subunit interface. In the reduced form Ni^{2+} is in a square planar in geometry and has an N_2S_2 donor set provided by the N terminal sequence His-Cys-Xaa-Xaa-Xaa-Cys. The proposed enzymatic mechanism involves the binding of superoxide at the nickel, followed by proton transfer and release of hydrogen peroxide. A second superoxide binds, another proton is transferred and dioxygen is released. Spectroscopic evidence, specifically EPR, supports the formation of Ni^{3+} during the catalytic cycle, stabilized by the binding of a His residue axially (Figure 1.2).^[14, 15, 16, 17]

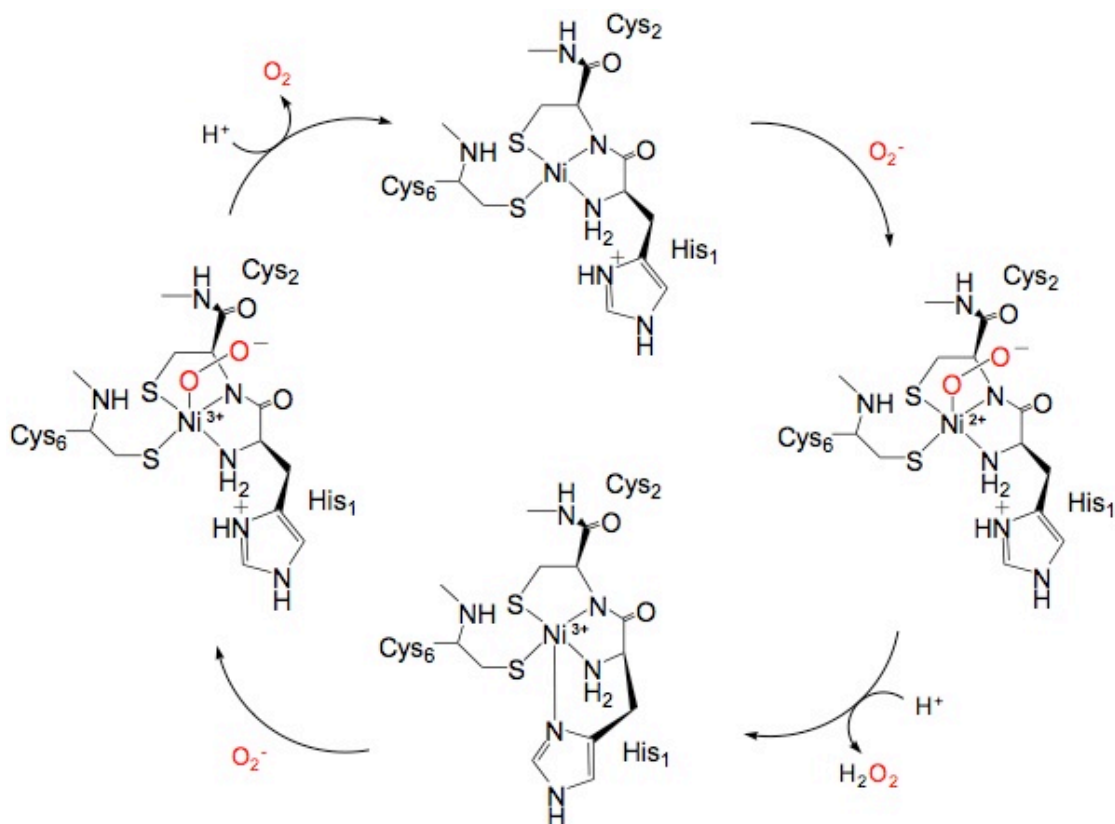


Figure 1.2 Proposed enzymatic mechanism for NiSOD.

Open questions regarding the mechanism of NiSOD remain. Although spectroscopic evidence has been gathered to support the formation of Ni³⁺ with imidazole binding, no direct spectroscopic evidence has provided information on the binding of superoxide. The source of the proton for the generation of hydrogen peroxide has also lead to some debate. There are three contenders for the source of the proton, a protonated nickel bound thiolate, an active site water, and the entry of a protonated superoxide.^[18, 19, 20] NiSOD is currently the only nickel containing enzyme believed to bind a form of dioxygen. The discovery of NiSOD and the incomplete

knowledge about the enzyme's mechanism have sparked further interest in the synthesis, characterization and reactivity of nickel-oxygen complexes.

1.2 Synthetic Mimics

Bioinorganic chemists commonly employ small molecules to help gain insight into the structure, spectroscopy, and mechanism of enzymes of interest. The rationale of exploiting model systems lies in our ability to control structure-function relationships. The identification, characterization, and reactivity of new structure types can lead to production of more accurate model systems, in hopes of elucidating details of an enzymatic mechanism. In this case, one could also envision developing new catalysts with SOD-like activity that would have a therapeutic effect. To date, there are a number of different nickel oxygen motifs that have been identified using small molecules (Figure 1.2).

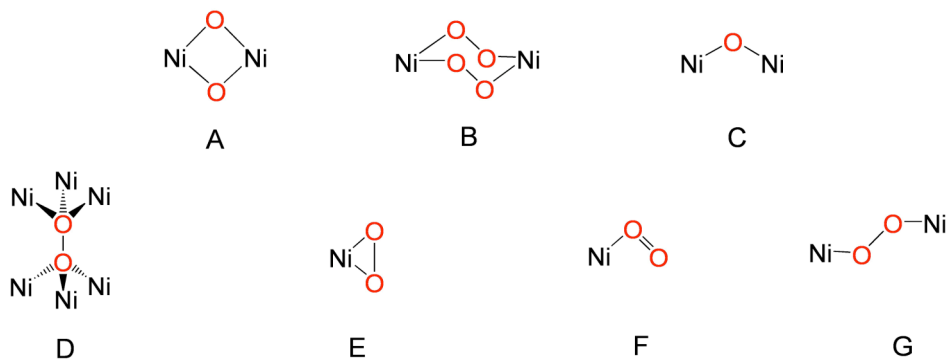


Figure 1.3 Nickel oxygen motifs^[21] A) bis(μ -oxo)^[22, 23, 24, 25] B) bis(μ -superoxo)^[23] C) μ -oxo^[26] D) μ_6 -peroxo^[27] E) “side-on” peroxo^[28] or “side-on” superoxo^[25, 29] F) “end-on” superoxo^[30] G) *trans*-peroxo^[31]

1.2.1 Nickel-Oxygen Complexes Formed from H_2O_2

The most common synthetic approach to the production of nickel-oxygen motifs employs the reaction of Ni^{2+} salts with hydrogen peroxide. The synthesis and identification of the first $\text{Ni}_2(\mu\text{-O})_2$ core was accomplished by such a route by Hikichi *et al.* in 1998.^[22] Reaction of the precursor, $[(\text{Tp}^{\text{iPr}})_2\text{Ni}_2(\mu\text{-OH})_2]$ ($\text{Tp}^{\text{iPr}} =$ hydrotris(3,5-diisopropylpyrazole)borate), with 1 equiv H_2O_2 in CH_2Cl_2 at low temperatures lead to an immediate color change from green to brown. The decomposition product was identified as the oxygen functionalization of an isopropyl substituent on each Tp ligand yielding an enolate bridged dimer (Figure 1.4). The instability of the complex derives from the ability to undergo hydrogen abstraction at the methyl position. This hypothesis was supported with the use of $[(\text{Tp}^{\text{Me}})_3\text{Ni}_2(\mu\text{-OH})_2]$ ($\text{Tp}^{\text{Me}} =$ hydrotris(3,4,5-trimethylpyrazolyl)borate) as the starting material,

which helped stabilize the $\text{Ni}_2(\mu\text{-O})_2$ complex, allowing for its identification and characterization.^[22-32]

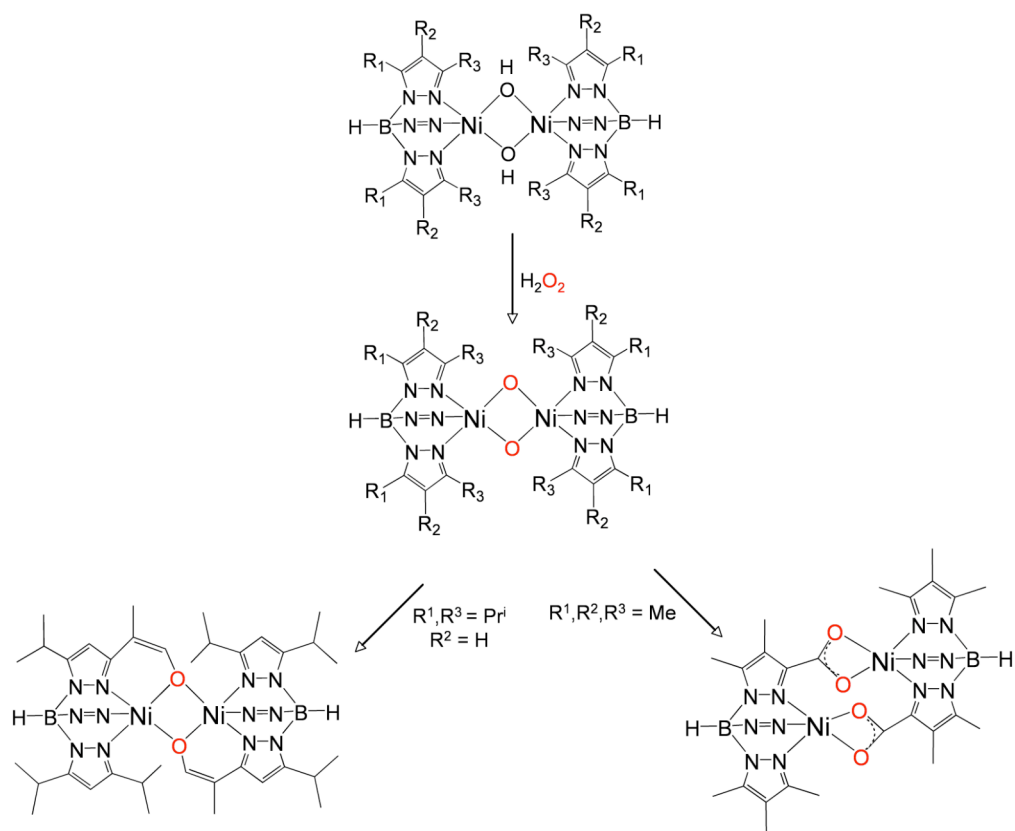


Figure 1.4 Formation of a bis(μ -oxo) complex leading to ligand oxidation.

1.2.2 Nickel-Oxygen Complexes Formed from Alternative Oxygen Atom Donors

There are a number of examples using H_2O_2 to obtain and study nickel oxygen complexes. However there are other oxidants in addition to H_2O_2 , which have the ability to donate a single oxygen atom, such as iodosylbenzene (PhIO). Such a system was employed by Kinnery *et al.* to demonstrate the first nickel-catalyzed epoxidation of an olefin using $[\text{Ni}(\text{tmc})](\text{NO}_3)_2$ as the catalyst.^[33] Epoxidation was observed with a variety of substrates including *trans*-1-phenyl-1-propene, *cis*-1-phenyl-1-propene, *trans*-1,1'-(1,2-ethenediyl)bis(benzene), and *cis*-1,1'-(1,2-Ethenediyl)bis(benzene). It was proposed that reaction of the nickel complex with PhIO leads to a powerful oxidant, thought to possibly be a terminal Ni-O species with considerable radical character, which then adds to the olefin to give an alkyl radical intermediate, followed by reductive elimination to give the epoxide (Figure 1.4).^[33] However, such intermediates have been identified.

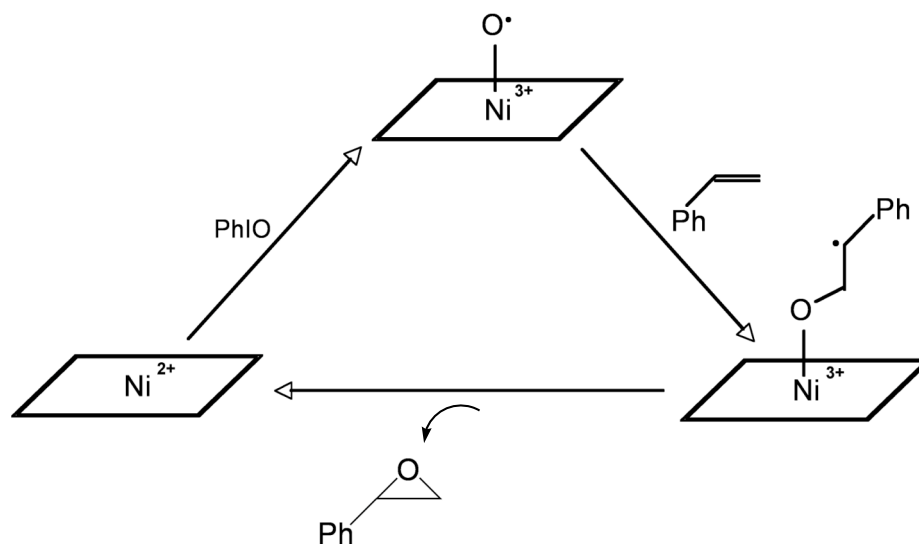


Figure 1.5 Epoxidation of an olefin by a nickel complex upon reaction with PhIO. Phenyl aldehyde was observed in low yields.

1.2.3 Nickel-Oxygen Complexes Formed from Dioxygen

Dioxygen, though readily available, is not often used as an oxidant because nickel complexes are generally inert toward dioxygen. The lack of reactivity is a result of the high $\text{Ni}^{3+}/\text{Ni}^{2+}$ redox couple (generally > 1 V), making Ni^{2+} complexes reactive only towards more reduced forms of dioxygen, e.g. peroxides and superoxides, as demonstrated above. Though uncommon, it is possible to design a ligand sufficiently electron rich, making reaction with dioxygen thermodynamically favorable. However, there is a limitation to this strategy. The electron rich ligand environment is also then susceptible to oxidation by the nickel-oxygen intermediates.

Kimura *et al.* designed a dioxo-pentaaza macrocycle that lowered the $\text{Ni}^{3+}/\text{Ni}^{2+}$ redox couple to 0.24 V(vs SCE), permitting reaction with dioxygen.^[34,35] Though unable to identify the details concerning the geometric and electronic features, the product of dioxygen addition was identified as a monomeric Ni^{3+} -superoxo complex based on quantification of dioxygen uptake, electronic absorption features, as well as magnetic and potentiometric measurements. The complex was the first intermediate derived from dioxygen activation by a Ni^{2+} complex. Reactivity studies indicated that the Ni-superoxo complex was competent in oxidizing aromatic substrates. Subsequent studies indicated that the major product of the reaction was ligand oxidation, demonstrating the limitation of an electron rich ligand system that permits reaction of the metal with dioxygen (Figure 1.6).^[34, 35]

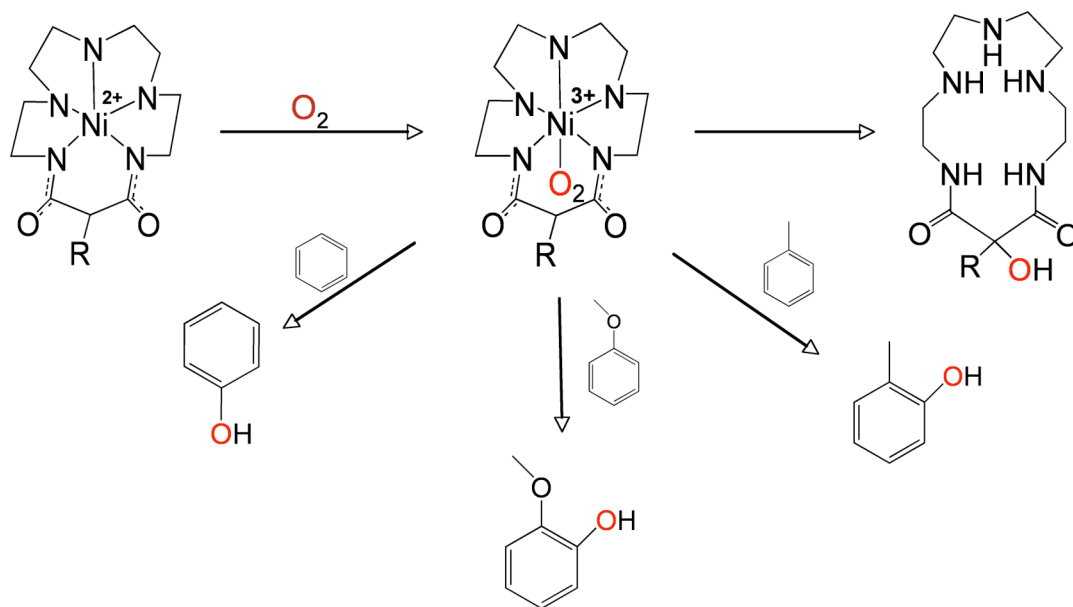


Figure 1.6 Activation of dioxygen with a Ni^{2+} complex capable of oxidizing aromatic substrates. The major product was ligand oxidation ($R = H, F, CH_2CH_3$, or $CH_2C_6H_5$).

To avoid ligand oxidation while still using dioxygen as the oxidant one can lower the oxidation state of the metal such that reaction with dioxygen readily occurs. In 1969, Otsuka *et al.* used a $Ni(0)$ source as a catalyst in the formation of cyanates from various alkyl isocyanides.^[28,36] Upon reaction with dioxygen, a green intermediate was observed which was identified as a “side-on” mononuclear $Ni(II)$ -peroxo species (Figure 1.7).^[28,36] It was subsequently characterized by X-ray diffraction analysis.

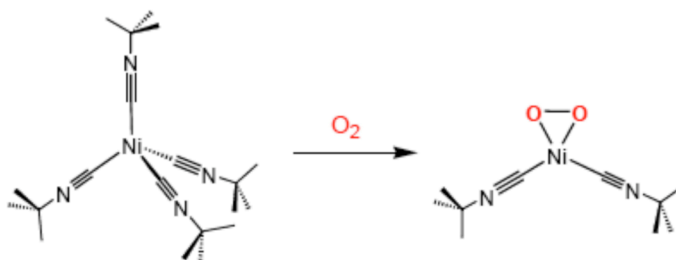


Figure 1.7 Activation of dioxygen by a Ni(0) complex to form a monomeric “side-on” peroxo complex.

Riordan and coworkers utilized the tris(thioether)borate ligand system (PhTt) to permit for the activation of dioxygen by Ni(I) complexes.^[37] The soft thioether ligation stabilizes the lower oxidation state. In addition, the substituent on the thioether arm can be readily modified, allowing the steric bulk to be altered as needed.^[38] Reaction of $[\text{PhTt}^{\text{R}}]\text{NiCO}$ (where R = Ad, ^tBu) with dioxygen has been extensively studied.^[24, 39] The steric demands of the ligand thioether substituent play a key role in determining the nickel oxygen products. With the less bulky substituent, *t*-butyl, a dark purple product was observed (Figure 1.8). This assignment of the bis(μ -oxo) dinickel(III) complex was difficult due to thermal instability. However, vibrational data, XAS, EXAFS, NMR, UV-Vis, and a low quality crystal structure confirmed the assignment.^[24, 39] Although this is not the first bis(μ -oxo) dinickel(III) dimer to be identified, it is the first derived from dioxygen.

Interestingly, when the steric bulk of the ligand is increased, a monomeric species is formed. Altering the substituent on the thioether arm has no effect on the

electronic properties of the ligand, as indicated by the absence of a change in the C=O stretching frequency for the $[\text{PhTt}^{\text{R}}]\text{Ni}(\text{CO})$ adducts, signifying the difference in reactivity towards dioxygen is sterically controlled. Reaction of $[\text{PhTt}^{\text{Ad}}]\text{Ni}(\text{CO})$ with dioxygen produced a brown complex which was identified as a “side-on” superoxo species. Importantly, it was demonstrated that the “side-on” superoxo species is an intermediate in the formation of the bis(μ -oxo) complex, observed with the *t*-butyl substituent.^[25, 40] Using $[\text{PhTt}^{\text{Ad}}]\text{NiCO}$ the “side-on” superoxo complex was synthesized and was then reacted with $[\text{PhTt}^{\text{tBu}}]\text{NiCO}$, giving rise to a bis(μ -oxo) dimer (Figure 1.8). Decomposition of the bis(μ -oxo) dinickel(III) complex produces oxygenated ligand products.

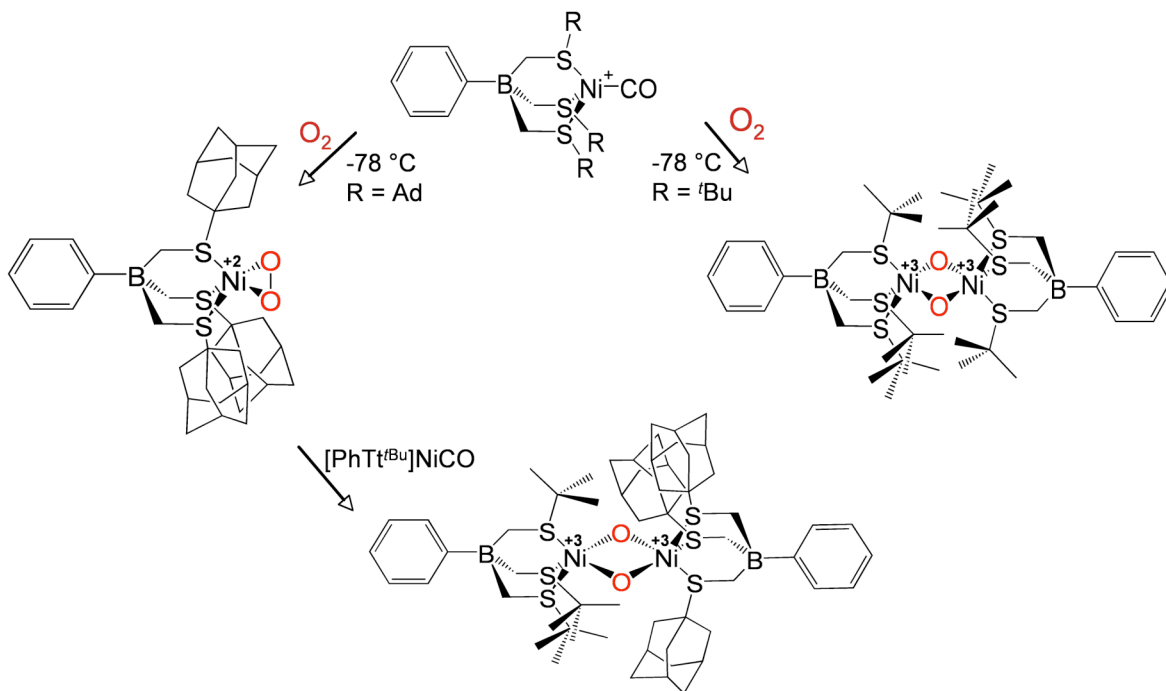


Figure 1.8 Summary of the activation of dioxygen by $[\text{PhTt}^{\text{R}}]\text{Ni}(\text{CO})$.^[21]

Through experimental data and DFT calculations a general understanding of the oxygen activation by $[\text{PhTt}^{\text{R}}]\text{Ni}(\text{CO})$ was established. First, dioxygen reacts with the nickel complex giving rise to a mononuclear “side-on” complex which, depending on ligand sterics, can then dimerize to form the bis(μ -oxo) dinickel(III). A plausible intermediate has been hypothesized as a (μ - η^2 : η^2) bridging peroxo, indicating dimerization prior to the breaking of the O-O bond. However, DFT calculations predict a μ - η^2 : η^2 -peroxo dinickel(III) species to be energetically unstable compared to the bis(μ -oxo) dinickel(III) species.^[21] Calculations indicate that the cleavage of

the O-O bond can arise from the effective nuclear charge of the nickel and more effective back donation that would weaken and break the O-O bond.^[21] Nevertheless, it remains unknown if other intermediates are involved in the bis(μ -oxo)dinickel(III) formation.

The most relevant work related to the studies in this thesis is that of Kieber-Emmons *et al.*^[21] With the objective of expanding the field of known nickel-oxygen motifs, the reaction of $[\text{Ni}(\text{TMC})]^+$ with dioxygen was assayed. Upon reaction with dioxygen at low temperatures an immediate color change is observed from a light blue to red. Though thermally unstable, spectroscopic evidence indicated the formation of a peroxo-bridged dinickel complex, $\{[\text{Ni}(\text{TMC})]_2(\mu\text{-O}_2)\}^{2+}$, a structure type previously unknown in nickel chemistry. Interestingly, it was determined that the formation of the dimer occurs under limiting amounts of dioxygen. When in the presence of excess oxygen, a monomeric “end-on” superoxo complex is obtained. The two complexes are in equilibrium with one another and that equilibrium lies largely towards the superoxo complex. The thermal decomposition product was identified as a $[\text{Ni}(\text{TMC})\text{OH}]^+$. Isotopic labeling studies deduced that the hydrogen is derived from the solvent, CH_3CN . It is unknown which nickel-oxygen complex is responsible for the hydrogen abstraction (Figure 1.8).^[21, 30, 31, 41] The Ni(TMC) system demonstrates the importance of using different oxygen sources while investigating metal oxygen systems. Though both hydrogen peroxide and dioxygen addition to Ni(TMC) precursors give rise to the “end-on” superoxo complex, the μ -peroxo dinickel(II) dimer is observed only in the presence of dioxygen. Therefore, a thorough

examination of the formation of various nickel-oxygen complexes must include dioxygen.

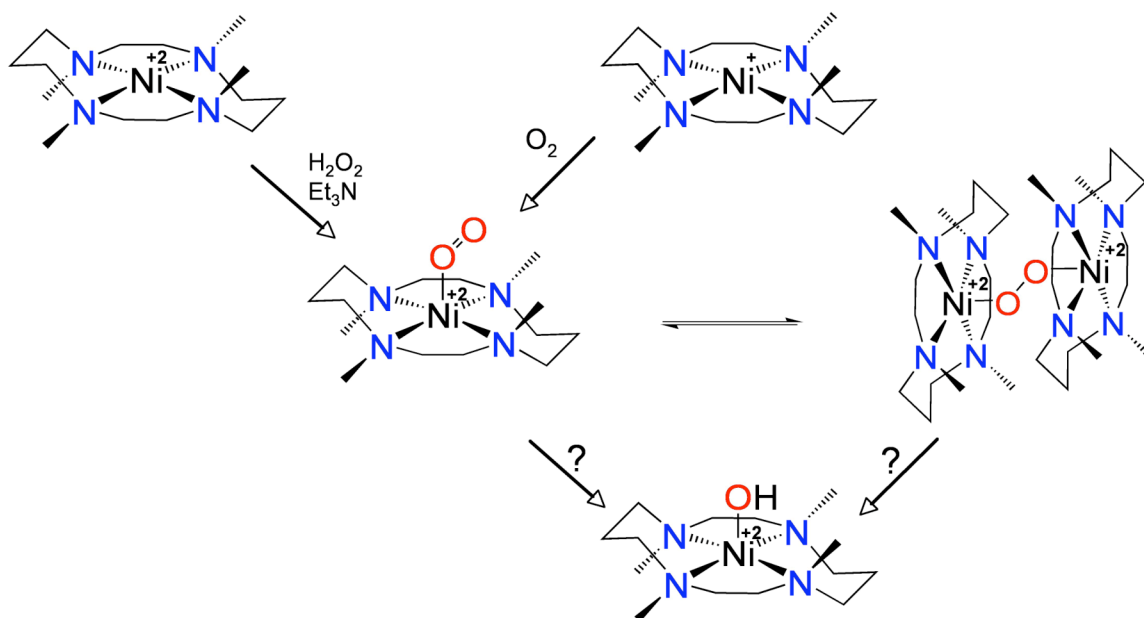


Figure 1.9 Summary of the activation of dioxygen by $[\text{Ni}(\text{TMC})]^+$.

1.3 Summary

Over hundreds of millions of years Nature has optimized the use of metals to active small molecules, including dioxygen. However, in synthetic chemistry the possibilities are just beginning to be uncovered. The study of nickel oxygen motifs remains largely unexplored, particularly those formed by reaction with dioxygen. The

examination of such systems can provide great insight in understanding basic biochemical reactions. The examples herein demonstrate the importance of structure-function relationships and contribute to understanding how to engineer future ligand systems. This thesis addresses the importance of the ligand system in obtaining new nickel-oxygen complexes and understanding their reactivity. The design and synthesis of new ligand systems as well as the oxygenation of nickel complexes through various routes is describe herein. The synthesis, characterization, and reactivity of the first “side-on” nickel(III)-peroxo complex derived from monovalent nickel and dioxygen is addressed.

CHAPTER 2

PHYSICAL METHODS AND LIGAND SYNTHESIS

2.1 Physical Methods

2.1.1 Nuclear Magnetic Resonance Spectroscopy

^1H and ^{13}C NMR spectra were acquired on either a Bruker AV 400 auto sampler or a Bruker DRX 400. Both spectrophotometers are outfitted with QNP probes. Air sensitive samples were prepared in either an Ar or N_2 glovebox, capped with a septum and sealed with parafilm or teflon tape.

2.1.2 Infrared Spectroscopy

Infrared data was collected on a Genesis Series FTIR spectrophotometer. The data was processed using the WinFIRST (1997) program. Solid samples were prepared by first flushing the sample chamber with N_2 and completing a background scan to ensure removal of atmospheric gases. In general, samples were ground to a fine powder with KBr using a mortar and pestle. The mixture was then placed in a pellet press. Air sensitive samples were prepared in a N_2 glovebox.

2.1.3 Mass Spectroscopy

Low-resolution mass spectra were recorded on a Finnegan LCQ spectrometer with electrospray injection. A small vial with the sample was placed in a larger vial and sealed under inert atmosphere. A sample aliquot was removed with a needle for a single injection to limit exposure to either oxygen or moisture.

2.1.4 Electronic Absorption Spectroscopy

Optical spectra were collected on a Varian Cary 50 spectrophotometer equipped with a fiber optic coupler and a Hellma quartz immersion probe, 1 cm path length. Optical data was first collected on solvent at a given temperature allowing for background correction. The sample cells are custom-made glass vessels constructed to exclude water or oxygen at lower temperatures. In a typical experiment samples were prepared in an Ar-filled glove box. The glass vessel was filled with approximately 10 mL of solution, sealed and removed from the glove box. Under a positive pressure of N₂ the immersion probe was inserted. The N₂ flow was stopped and data was acquired. If additional gases or reagents were needed, a positive pressure of N₂ was reintroduced and the gas/reagent was added via a needle through a rubber septum in a sidearm.

2.1.5 Electron Paramagnetic Resonance Spectroscopy

Electron paramagnetic resonance spectroscopy was performed at the University of Wisconsin-Madison. A Bruker ELEXSYS E 500 spectrometer equipped with an Oxford ESR 900 continuous flow liquid helium cryostat, and Oxford ITC4 temperature controller, and a Bruker SuperX-CW frequency counter were utilized for data collection. Frank Neese's WEPR program was used to simulate the spectra.^[42] Dioxygen was added to the sample EPR tube via a needle and was bubbled through the solution for approximately 30 seconds. Dioxygen flow was ceased and the headspace evacuated under vacuum and back filled with N₂. The samples were then placed in a pre-cooled Dewar for shipping.

2.1.6 X-Ray Diffraction

Crystals were mounted and solved by Dr. Glenn Yap, University of Delaware. Data was collected on a Bruker-AXS APEX CCD diffractometer with 0.7107 Å Mo K_α radiation. The SADABS program was used for absorption correction. The SHELXTL 6.12 program provided information regarding systemic absences allowing the structure to be solved in the appropriate space group.

2.1.7 Gas Chromatography

Gas chromatography data was collected on a Varian CP-3800 Gas Chromatograph coupled with a Varian Saturn 2000 mass spectrometer. General parameters used included a 200°C injection temperature and a starting column temperature of 50°C followed by a ramp to 300°C at 10°C/minute.

2.2 Experimental

All solvents were purchased at reagent grade of higher. Solvents were dried by passage through an activated alumina column. Air sensitive samples were prepared in either an Ar or N₂-filled glovebox

2.2.1 Synthesis of Tetraneopenyl Cyclam

Cyclam was prepared following the report by Barefield and co-workers.^[43] Tetraneopentyl cyclam (TNPC) was prepared in a manner adapted from Sibert and co-workers.^[44] A typical synthesis involved adding dry CH₂Cl₂ (~50 mL) to 1.0 g (0.005 mol, 1 eq) of cyclam under an inert atmosphere. 5.0 g (0.05 mol, 10 eq) of Et₃N was added. The mixture was stirred for 15 min before 2.4 g (0.02 mol, 4 eq) of trimethylacetyl chloride was added. The mixture was stirred further for 30 minutes producing a homogenous colorless solution. The mixture was concentrated and the

excess Et₃N was removed by water extraction. The organic layer was dried over magnesium sulfate, filtered, and the solvent was removed giving a white solid identified as tetrapivaloyl cyclam (Figure 2.1). Yield = 80%. ESI-MS *m/z*: 537 (M+H)⁺. ¹H-NMR (400 MHz, CDCl₃) δ = 1.25 (s, CH₃ neopentyl, 36H), 1.91 (b, propyl, 4H), 3.44 (b, propyl amine, 8H), 3.52 (b, ethyl amine, 8H). ¹³C-NMR (400 MHz, CDCl₃) δ = 28.0 (CH₃-neopentyl), 38.5 (CH₂ –ethyl amine, propyl amine), 46.8 (CH₂-propyl), 48.2 (C-neopentyl) 177.5 (C=O-neopentyl).

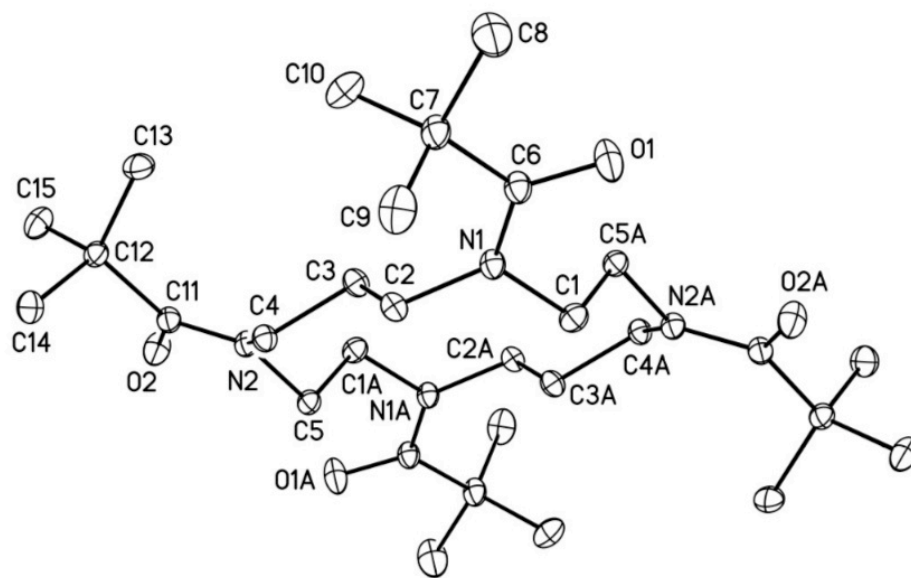


Figure 2.1 Structure of tetrapivaloyl cyclam as determined by X-ray diffraction. Thermal ellipsoids drawn at 30%. Hydrogen atoms not shown.

A solution of lithium aluminum hydride (425 mg, 0.011 mol, 6 eq) in dry THF was cannula transferred to a tetrapivaloyl cyclam (1.0 g, 0.0019 mol, 1 eq) solution

(~50 mL dry CH₂Cl₂) at -78 °C. The solution was warmed to room temperature and stirred for 4 hours. The reaction mixture was quenched with ethanol and water, filtered through Celite, and the solvent removed under vacuum. Water was added, the layers separated, and the organic layer was dried over magnesium sulfate, filtered, and the solvent was removed giving a white solid (Figure 2.2). Yield = 82%. ESI-MS *m/z*: 481 (M+H)⁺. ¹H-NMR (400 MHz, CDCl₃) δ = 0.76 (s, CH₃ neopentyl, 36H), 1.59 (q, propyl, 4H), 2.05 (s, CH₂ neopentyl, 8H), 2.49 (b, ethyl amine, propyl amine, 16H). ¹³C-NMR (400 MHz, CDCl₃) δ = 21.1 (CH₂-propyl), 27.0 (CH₃-neopentyl), 32.0 (CH-neopentyl), 51.8 (CH₂-ethyl amine), 53.2 (CH₂-propyl amine), 67.9 (CH₂-neopentyl).

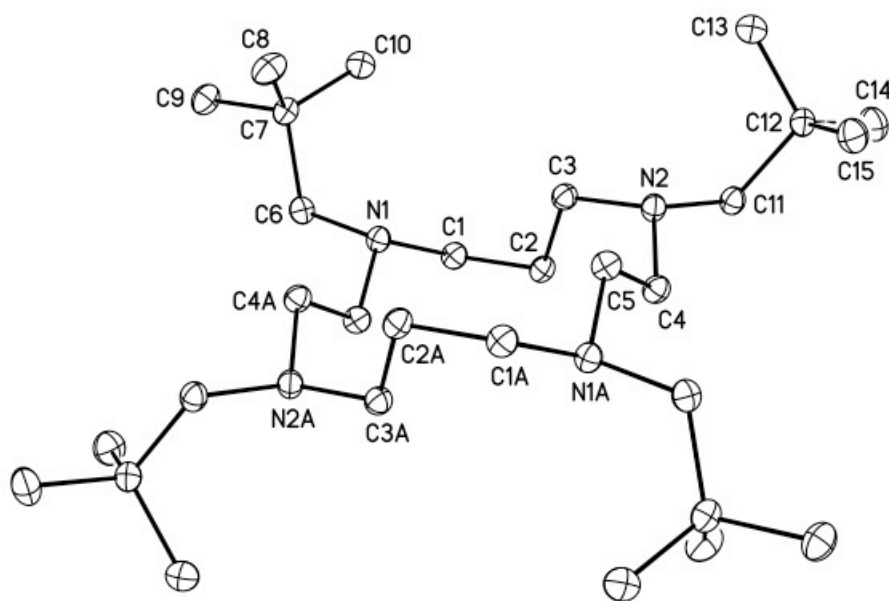


Figure 2.2 Structure of TNPC as determined by X-ray diffraction. Thermal ellipsoids drawn at 30%. Hydrogen atoms not shown.

2.2.2 Metal-Based Oxidative Decomposition of TNPC

A solution of TNPC in DMF was added dropwise to a solution of $\text{Cu}(\text{H}_2\text{O})_6\text{Cl}_2$ and refluxed under an ambient atmosphere for 6 hours. The solution was filtered and unreacted TNPC was removed. The orange filtrate contained the oxidized decomposition product. Crystals were obtained by slow evaporation of CH_2Cl_2 . ESI-MS m/z : 237.3 ($\text{M}+\text{H}$)⁺. IR: $\nu_{\text{CN}} = 1571 \text{ cm}^{-1}$. ^1H -NMR (400 MHz, CDCl_3) δ = 0.91 (s, neopentyl, 18H), 2.06 (b, ethyl amine, neopentyl, 8H), 5.01 (t, propyl, 1H), 7.61 (d, propyl amine, 2H).

2.2.3 Synthesis of $[\text{Pd}(\text{TNPC})]\text{Cl}_2$

The synthesis of the $[\text{Pd}(\text{TNPC})]\text{Cl}_2$ was completed by dissolving TNPC (0.5 g, 1.04 mM, 1 eq) in dry THF in an anaerobic environment. A THF solution of $\text{PdCl}_2 \cdot (\text{CH}_3\text{CN})_2$ (0.27 g, 1.04 mM, 1 eq) was added dropwise to the TNPC solution. The solution was stirred for ~ 10 hours at room temperature giving rise to an olive-green precipitate, which was filtered and preliminarily identified as $[\text{Pd}(\text{TNPC})]\text{Cl}_2$, with an average yield of 40%.

2.2.4 Synthesis of [Ni(tmcyclen)](OTf)₂

[Ni(tmcyclen)](OTf)₂ was prepared in a manner similar to that reported by Coates *et. al.*^[46] 1,4,7,10-tetraazacyclododecane (cyclen) was purchased from Strem (99%, CAS: 294-90-6). Methylation was accomplished by refluxing 1g of cyclen (5.8 mmol), 5.3 mL formic acid (98-100%), 4.4 mL formaldehyde (37 %), and 0.5 mL water for 72 hours. The reaction mixture was then transferred with ~25 mL water to a 250-mL beaker and cooled in an ice bath. A concentrated solution of KOH (15 g into 50 mL water) was added slowly. The product was extracted with CHCl₃, dried over magnesium sulfate, filtered, and the solvent removed. If impurities remained the ligand was distilled under vacuum.

Pure ligand was re-dissolved in ethanol and added dropwise to an aqueous solution of Ni(OTf)₂. The mixture was refluxed for 4 hours resulting in a color change from green to red. The solution was allowed to cool overnight and filtered through a fine porosity frit. The solvent was removed under vacuum and the product was recrystallized from acetone.

2.3 Ligands

Herein, three different ligands were utilized. The first complex is [Ni(TMC)]⁺, mentioned in the Introduction Chapter, which has been studied previously in the Riordan lab. A second macrocycle, tetraneopentyl cyclam, should provide similar electronic characteristics but should sterically hinder dimer formation. Lastly, the

tmcyclen macrocycle could give rise to new nickel-oxygen structures. These ligands should provide fundamental information on the structure-function relationships in nickel-oxygen chemistry.

2.3.1 Tetraneopentyl Cyclam

Thermal decomposition of $[\text{Ni}(\text{TMC})(\text{O}_2)]^+$ gives rise to $[\text{Ni}(\text{TMC})\text{OH}]^+$. The source of the hydrogen was demonstrated to be the solvent, CH_3CN , by isotopic labeling studies.^[10] However, the ability to determine which complex, either the “end-on” superoxo or the μ -peroxo dinickel(II), gives rise to the hydrogen abstraction was hindered due to the equilibrium between the two species. Thus, reactivity studies with this system, though informative, would not provide direct evidence as to which complex is responsible for the reactivity observed. In order to study the reactivity of one species it must be formed independent of the other. To accomplish this a new ligand was designed. The working hypothesis is that the TNPC macrocycle would provide similar electronic characteristics, leading to the formation of the “end-on” superoxo complex, but would sterically hinder the formation of the peroxo dimer.

2.3.1.1 Attempted Metallation of TNPC

Metallation of tetraaza macrocycles is commonly accomplished by combining the desired metal salts with the ligand in a mixed solvent system.

Metalation of the TNPC macrocycle was attempted with nickel under a variety of conditions to no avail. Nickel sources that were utilized included NiCl_2 , $\text{Ni}(\text{NO}_3)_2$, $\text{NiCl}_2(\text{THF})$, and $\text{Ni}(\text{OTf})_2$. A solution of the nickel salt was added dropwise to a solution of TNPC and refluxed under an ambient atmosphere for 8 hrs in various solvent mixtures including $\text{CHCl}_3/\text{EtOH}$, DMF, THF, and THF/EtOH. In all cases, excluding the reaction completed in refluxing DMF, free ligand was recovered. The product of the reaction in DMF gave rise to a new feature in the infrared spectrum at 1661 cm^{-1} , indicating possible ligand decomposition. Under anaerobic conditions all attempted syntheses were unsuccessful yielding only unreacted starting material, even in refluxing DMF.

In addition to nickel other transition metals were investigated including Cu, Fe, and Pd. Copper(II) displayed the same trend as Ni, where only free ligand was recovered. Under anaerobic conditions with refluxing DMF no metalation was observed, however, metalation in DMF under O_2 resulted in a color change to yellow and a new feature was identified in the infrared spectrum at 1571 cm^{-1} . Metalation attempts with Fe were also unsuccessful. Reaction of TNPC with $\text{PdCl}_2 \cdot (\text{CH}_3\text{CN})_2$ showed ligand decomposition under aerobic conditions indicated by a new feature in the infrared spectrum at 1603 cm^{-1} . However, under anaerobic conditions metalation with Pd was accomplished. Two different alkylation methods of tetraaza macrocycles have been reported.^[43] The first entails the alkylation of the macrocycle which is then metalated, as described above. Alternatively, alkylation has been described on a metalated macrocycle.^[43] However, attempts to alkylate $[\text{Ni}(\text{cyclam})]^{2+}$ with either pivaloyl chloride or neopentyl chloride were also unsuccessful.

Metalation was observed when the second row transition metal palladium was employed giving rise to $[\text{Pd}(\text{TNPC})]\text{Cl}_2$. Electronic absorption spectroscopy shows a feature at $\lambda_{\text{max}} = 320$ nm and another at 405 nm. However, accurate quantification was not possible due to the low solubility and compound precipitation. The neopentyl methyl signal in the ^1H NMR spectrum is shifted downfield from $\delta = 0.75$ to 1.17 upon metal binding. Mass spectral analysis confirmed the presence of $[\text{Pd}(\text{TNPC})]\text{Cl}_2$ with a monoisotopic mass of 658.3 consistent with $(\text{M} + \text{H})^+$ (Figure 2.3).

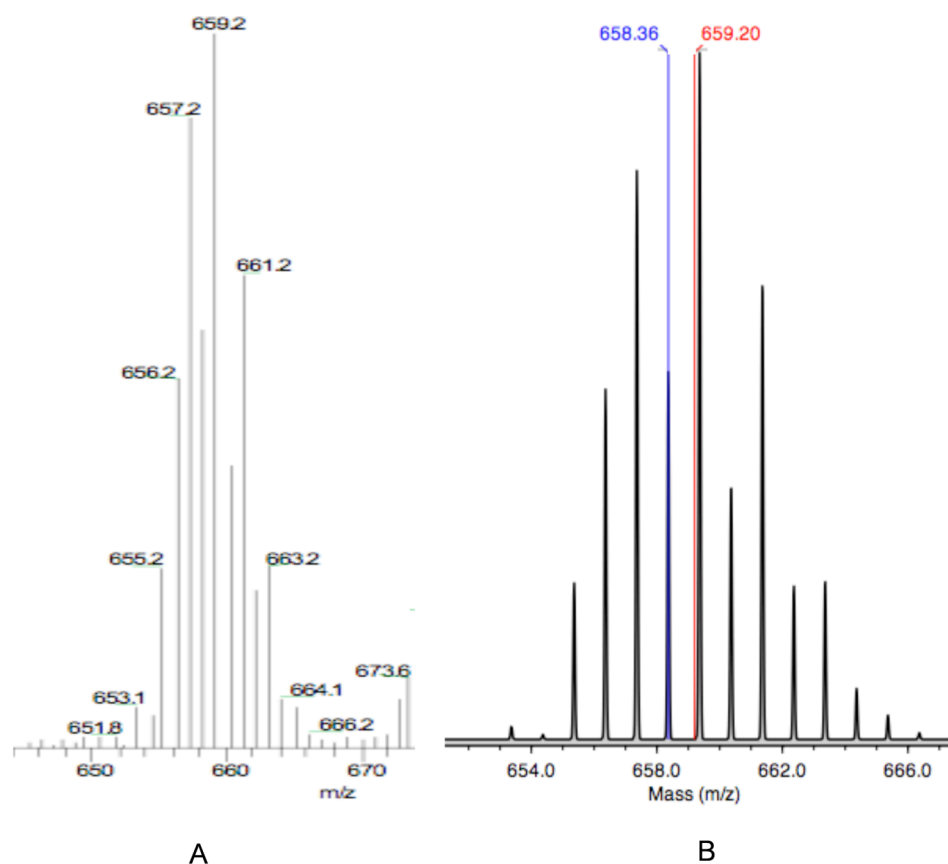


Figure 2.3 Mass Spectral data for [Pd(TNPC)]Cl₂. A) Experimental ESI-MS spectrum with $m/z = 659.2$ ($M+H$)⁺ B) Theoretical Isotopic distribution pattern for ([Pd(TNPC)]Cl₂+H)⁺. --- Average mass --- Monoisotopic mass.

2.3.1.2 Metal-Mediated Oxidative Decomposition of TNPC

The inability to obtain metal complexes of TNPC with Cu, Fe, or Ni was not entirely unexpected. A previous study reported the inability of cyclam macrocycles to bind Ni or Cu when sterically demanding substituents, such as benzyl or isopropyl,

were employed.^[45] However, when second row transition metals are used the reaction becomes thermodynamically favorable as demonstrated by the formation of $[\text{Pd}(\text{TNPC})]\text{Cl}_2$. Under aerobic conditions reaction of TNPC with CuCl_2 yielded a new product as evidenced first by its infrared spectrum. The product was crystallographically characterized showing the TNPC macrocycle had undergone metal-mediated oxidative decomposition (Figure 2.4 and Figure 2.5). Attempts to design a more sterically hindered cyclam macrocycle were successful. However, binding of first row transition metals is thermodynamically unfavored in these systems. Moreover, the TNPC macrocycle is susceptible to metal-promoted decomposition at higher temperatures in the presence of air.

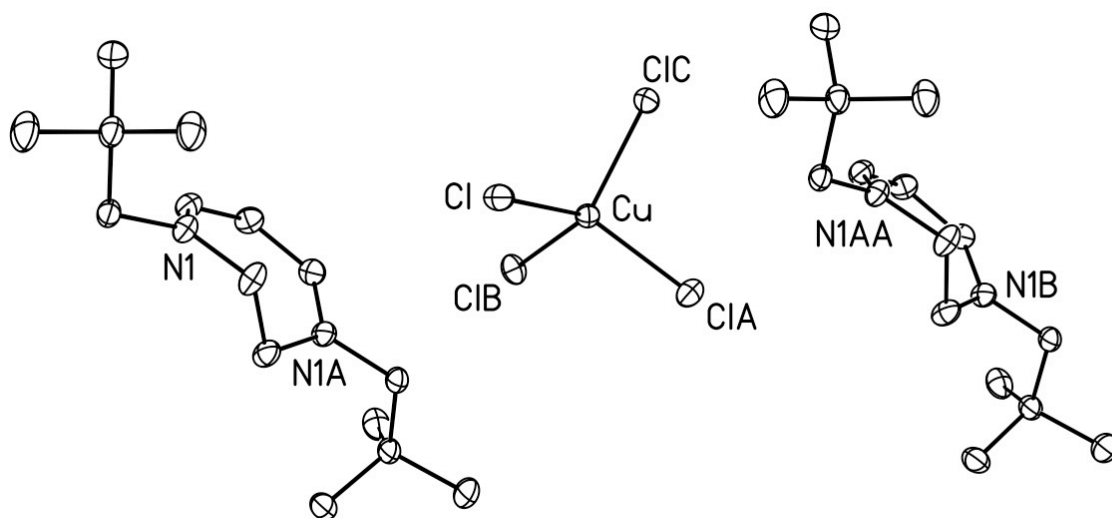


Figure 2.4 Oxidative decomposition product of TNPC. Two macrocycles co-crystallized with CuCl_4^{2-} per unit cell. Thermal ellipsoids drawn at 30%. Hydrogen atoms not shown.

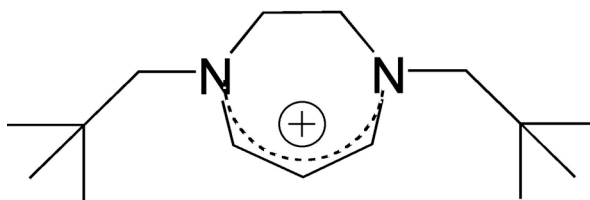


Figure 2.5 Oxidative decomposition product of TNPC, included for clarity.

2.3.2 The Tmcyclen Macrocycle

The synthesis of $[\text{Ni}(\text{tmcyclen})]^{2+}$ was first reported by Coates *et al.* in 1982.^[46] However, the ligand had not been employed in nickel oxygen chemistry previously. The tmcyclen ligand provides a number of features that were attractive for our purposes. Tmcyclen has similar electronic characteristics, to TMC, but provides a smaller cavity, which is targeted to help stabilize metals in higher oxidation states. The known *R,S,R,S* isomer has all four methyl substituents positioned on one face of the macrocycle. Having all methyl substituents on one face could sterically hinder dimer formation upon dioxygen activation, if dioxygen activation with $[\text{Ni}(\text{tmcyclen})]^+$ were comparable to that of $[\text{Ni}(\text{TMC})]^+$. Lastly, metalation of the macrocycle has been reported, even when larger substituents, such as benzyl were employed.^[47] Therefore, tmcyclen was deemed an appropriate candidate to aid in the exploration of nickel(I)-dioxygen chemistry.

2.3.2.1 Synthesis of [Ni(tmcyclen)](OTf) and [Ni(tmcyclen)(CO)](OTf)

Due to the inherent lack of reactivity of most Ni^{2+} complexes towards dioxygen, one electron reduction of $[\text{Ni}(\text{tmcyclen})]^{2+}$ using a sodium-mercury amalgam was conducted. Approximately, 20 mL of THF was added to a 0.5% Na/Hg amalgam followed by 200 mg of $[\text{Ni}(\text{tmcyclen})]^{2+}$. The heterogeneous solution was stirred for 20-25 minutes. The solution was then filtered through Celite, resulting in a pale yellow solution. $[\text{Ni}(\text{tmcyclen})](\text{OTf})$ appeared extremely sensitive to trace amounts of water, more so than $[\text{Ni}(\text{TMC})]^+$. Therefore it was difficult to work with or store. Due to the apparent instability of $[\text{Ni}(\text{tmcyclen})]\text{OTf}$, the CO adduct was sought. CO was bubbled through a THF solution of the freshly reduced complex for approximately five minutes, and a solution was stirred ~1 hour. Following solvent removal, the green product was recrystallized, yield = 45%, by vapor diffusion of pentane into a concentrated THF solution of $[\text{Ni}(\text{tmcyclen})(\text{CO})]\text{OTf}$.

Infrared spectroscopy is an important diagnostic tool for carbonyl complexes because the ν_{CO} band provides information as to the oxidation state of the metal. The solid state IR spectrum of $[\text{Ni}(\text{tmcyclen})(\text{CO})]\text{OTf}$ has a strong peak at 1964 cm^{-1} indicative of a Ni(I)-CO complex. The electronic absorption spectrum shows maxima at 425 ($\epsilon = 250\text{ L mol}^{-1}\text{ cm}^{-1}$) and 696 ($\epsilon = 50\text{ L mol}^{-1}\text{ cm}^{-1}$) which are similar to previously reported values for $[\text{Ni}(\text{TMC})(\text{CO})]^+$ of 450 ($\epsilon = 680\text{ L mol}^{-1}\text{ cm}^{-1}$) and 706 ($\epsilon < 100\text{ L mol}^{-1}\text{ cm}^{-1}$).^[48] The stronger ligand field of the smaller macrocycle explains the slight shift to higher energies. A low quality crystal structure of $[\text{Ni}(\text{tmcyclen})(\text{CO})]\text{OTf}$ was obtained (Figure 2.5). Prior reports of

$[\text{Ni}(\text{tmcyclen})\text{CO}]^+$ include its postulated existence during electrochemical examination of $[\text{Ni}(\text{tmcyclen})(\text{H}_2\text{O})]^{2+}$ under an atmosphere of CO. However, this is the first report of the isolation and full characterization of $[\text{Ni}(\text{tmcyclen})(\text{CO})]\text{OTf}$.^[49]

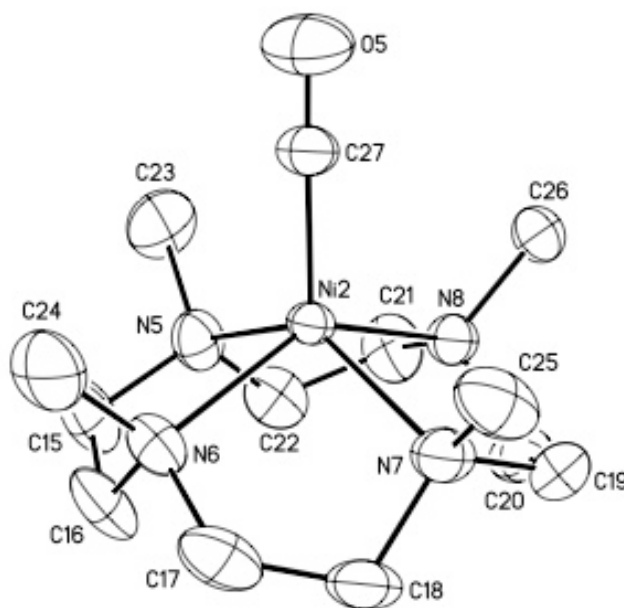


Figure 2.6 Crystal structure of $[\text{Ni}(\text{tmcyclen})(\text{CO})](\text{OTf})$. Thermal ellipsoids drawn at 30%. Hydrogen atoms and OTf anion not shown.

2.4 Summary

A sterically demanding macrocycle, TNPC, was synthesized with the objective of limiting the formation of dimers upon reaction of $[\text{Ni}(\text{TNPC})]^+$ with dioxygen. However, the synthesis of first row transition metal derivatives with this sterically

hindering substituent proved unsuccessful, presumably due to unfavorable thermodynamics. In light of these results an alternative macrocycle was employed, tmcyclen. The smaller macrocycle provided a number of beneficial characteristics including the ability to synthesize nickel macrocycles with larger substituents. This would allow for increased control over the steric and electronic properties of the nickel macrocycles. The oxygenation of the $[\text{Ni}(\text{tmcyclen})]$ was explored using different oxygenation sources. The reaction of $[\text{Ni}(\text{tmcyclen})](\text{OTf})_2$ with H_2O_2 as well as the activation of O_2 by $[\text{Ni}(\text{tmcyclen})(\text{CO})]\text{OTf}$ was explored. The oxygenation reactions lead to the identification of a “side-on” nickel(III)-peroxo complex.

CHAPTER 3

SYNTHESIS AND REACTIVITY OF [Ni(TMCYCLEN)(O₂)]OTf

3.1 Synthesis of [Ni(tmcyclen)(O₂)]OTf

Reaction of [Ni(tmcyclen)](OTf)₂ with 10 equivalents H₂O₂ in the presence of 10 equivalents of triethylamine produced a green intermediate which exhibited absorption features distinct from either [Ni(tmcyclen)](OTf)₂ or [Ni(TMC)(O₂)]OTf (Figure 3.1).^[30] The electronic absorption spectrum displays features at 347 nm ($\epsilon = 172 \text{ L}\cdot\text{mol}^{-1}\text{cm}^{-1}$), 398 nm ($\epsilon = 142 \text{ L}\cdot\text{mol}^{-1}\text{cm}^{-1}$), 639 nm ($\epsilon = 56 \text{ L}\cdot\text{mol}^{-1}\text{cm}^{-1}$), and 918 nm ($\epsilon = 40 \text{ L}\cdot\text{mol}^{-1}\text{cm}^{-1}$). The intermediate is produced in MeOH or CH₃CN.^[50]

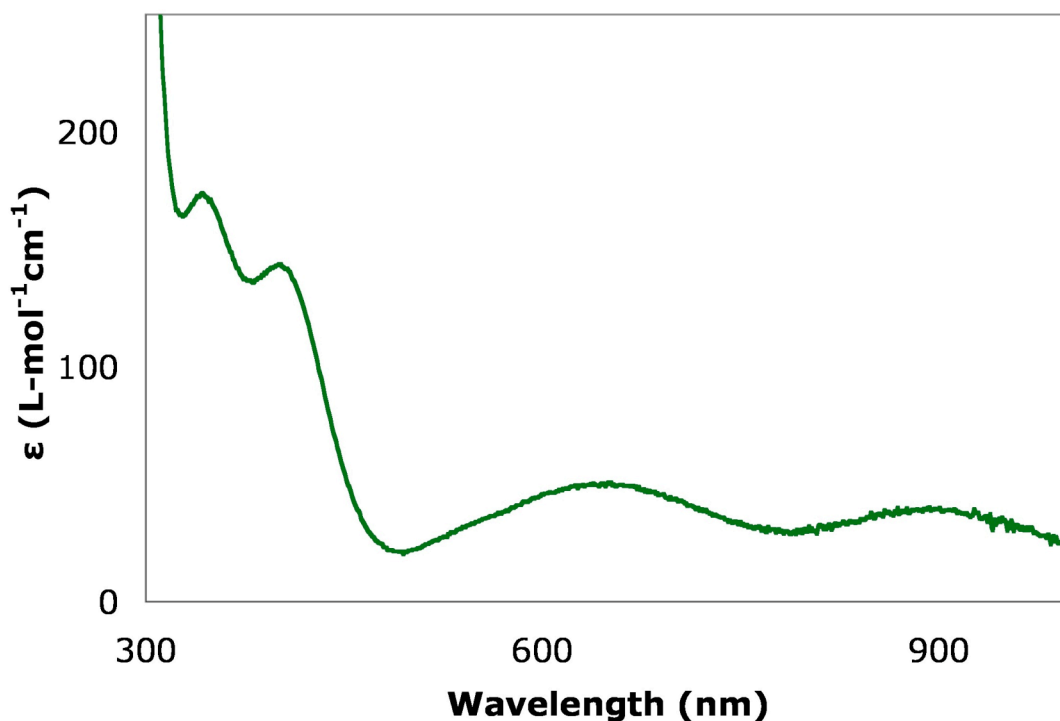


Figure 3.1 Electronic absorption spectrum of $[\text{Ni}(\text{tmcyclen})(\text{O}_2)\text{OTf}]$ in CH_3CN .

This thermally stable intermediate gave rise to a feature in the ESI-MS with a mass to charge (m/z) ratio of 318.0 corresponding to the parent ion $[\text{Ni}(\text{tmcyclen})(\text{O}_2)]\text{OTf}$. The calculated monoisotopic mass for a $[\text{Ni}(\text{tmcyclen})\text{O}_2]\text{OTf}$ species is $m/z = 318.16$. The mass spectroscopic data indicate the formation of a monomer. However, information regarding the nickel oxidation state and geometry required further investigation. Concurrent with this investigation an article was published which identified $[\text{Ni}(\text{tmcyclen})(\text{O}_2)]\text{ClO}_4$ as a “side-on” peroxo complex. Cho *et al.* published the synthesis of $[\text{Ni}(\text{tmcyclen})\text{O}_2]\text{ClO}_4$ using five equivalents of H_2O_2 and two equivalents of triethylamine in CH_3CN . The

absorption spectrum and the ESI-MS data indicate that the intermediate is the same in both cases.^[50]

Cho *et al.* published EPR data of this species that showed a rhombic signal with g values of 2.22, 2.17, and 2.06 at 4.3 K. This data is consistent with either a nickel(III)-peroxo or nickel(II)-superoxo adduct. A magnetic moment of $\mu_{\text{eff}} = 2.13 \mu_{\text{B}}$ was determined in further support of a ground state of $S = 1/2$. Resonance Raman data revealed an oxygen isotope sensitive band at 1002 cm^{-1} , which shifted to 945 cm^{-1} when the adduct was prepared from $\text{H}_2^{18}\text{O}_2$. The OO stretching frequency is lower than that observed for $[\text{Ni}(\text{TMC})(\text{O}_2)]^+$ (1131 cm^{-1}), indicating the former complex has a more reduced O_2 ligand. The Ni K-edge X-ray absorption spectral pre-edge transition occurs at 8332.3 eV. The pre-edge feature for $[\text{Ni}(\text{TMC})(\text{O}_2)]^+$ is 8331.6 eV, indicating a significant increase in nuclear charge in the former species consistent with a nickel(III) formulation. EXAFS data indicated a six coordinate nickel, indicative of a “side-on” complex. The above data suggest the formation of a six coordinate Ni(III) “side-on” peroxo complex. This was confirmed by an X-ray structure of $[\text{Ni}(\text{tmcyclen})(\text{O}_2)]\text{ClO}_4$. The OO bond distance of $1.386(4) \text{ \AA}$, is considerably longer than the OO bond length of $[\text{Ni}(\text{TMC})(\text{O}_2)]^+$ of 1.301 \AA determined by DFT methods, again indicating substantial peroxo character in the former species (Figure 3.2).^[50]

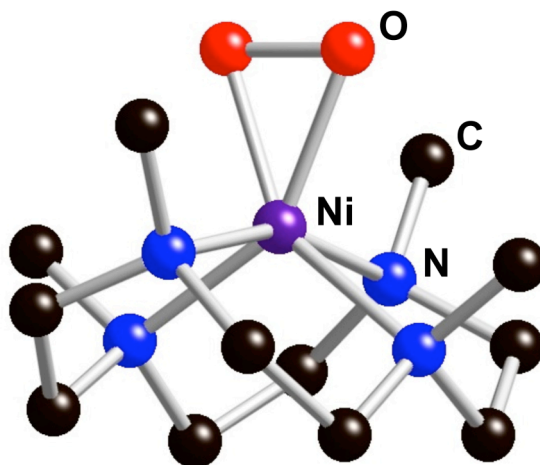


Figure 3.2 Structure of $[\text{Ni}(\text{tmcyclen})(\text{O}_2)]^+$ as determined by Cho *et. al.*

Reaction of potassium superoxide with $[\text{Ni}(\text{tmcyclen})](\text{OTf})_2$ also gave rise to similar features in the absorption spectrum (Figure 3.5), denoting the formation of the $[\text{Ni}(\text{tmcyclen})(\text{O}_2)]\text{OTf}$. A stock solution of 3 mM KO_2 in DMSO was added to a DMSO solution of $[\text{Ni}(\text{tmcyclen})](\text{OTf})_2$, resulting in an immediate color change to green consistent with the formation of $[\text{Ni}(\text{tmcyclen})(\text{O}_2)]\text{OTf}$.

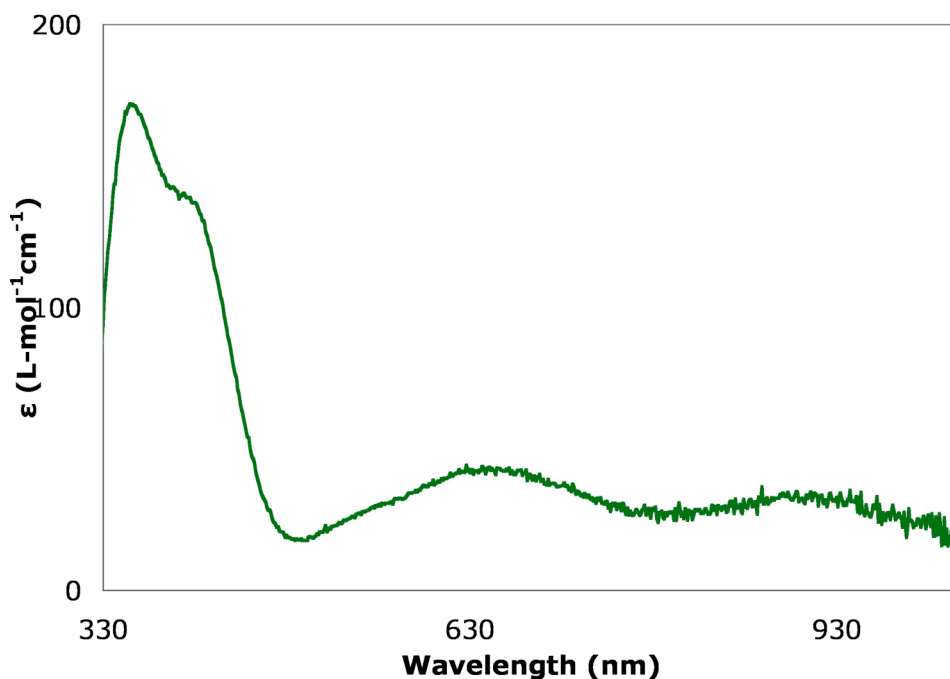


Figure 3.3 Electronic absorption spectrum of $[\text{Ni}(\text{tmcyclen})\text{O}_2]\text{OTf}$ formed via reaction of $[\text{Ni}(\text{tmcyclen})](\text{OTf})_2$ and KO_2 in DMSO.

3.2 Activation of O_2 by $[\text{Ni}(\text{tmcyclen})]\text{OTf}$

As aptly demonstrated by $[\text{Ni}(\text{TMC})]$, oxygenation of a complex via different routes can lead to the identification of different products. In order to determine if the $[\text{Ni}(\text{tmcyclen})]$ system behaved in a similar manner, oxygenation was investigated using O_2 . Dioxygen was bubbled through a THF solution of $[\text{Ni}(\text{tmcyclen})(\text{CO})]\text{OTf}$ at 25°C and the reaction course was monitored spectroscopically. Absorption features identical to the features identified as the Ni(III)-peroxo complex were evident (Figure

3.4). No intermediates were detected at room temperature as indicated by the clear isosbestic points. The rate of conversion from $[\text{Ni}(\text{tmcyclen})(\text{CO})]\text{OTf}$ to $[\text{Ni}(\text{tmcyclen})(\text{O}_2)]\text{OTf}$ at low temperature was such that no intermediate was detected. Preliminary experiments entailing oxygenation of $[\text{Ni}(\text{tmcyclen})]\text{OTf}$, low temperature gave no indication of additional intermediates.

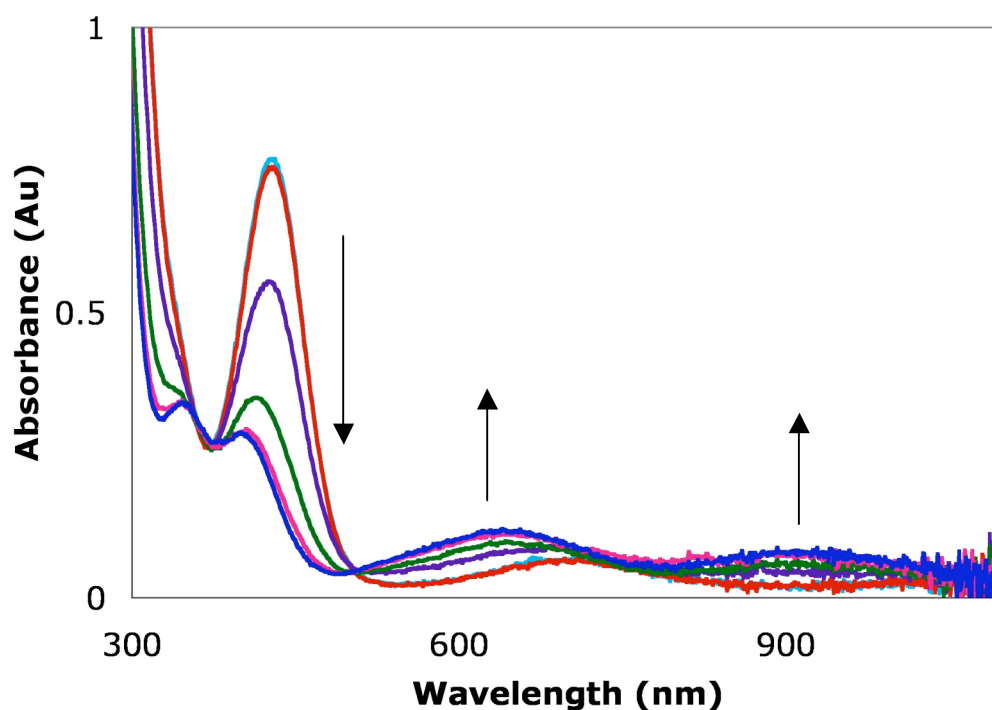


Figure 3.4 Electronic absorption spectrum showing the decrease of the $[\text{Ni}(\text{tmcyclen})(\text{CO})]\text{OTf}$ complex, giving rise to features assigned to the $[\text{Ni}(\text{tmcyclen})(\text{O}_2)]\text{OTf}$. Scans taken every 60 seconds.

ESI-MS data showed the identical feature at $m/z = 318.0$ that was observed for the product formed via reaction of the nickel(II) complex with H_2O_2 . In addition, the

EPR spectrum of a sample prepared via oxygenation of nickel(I) displayed a rhombic signal with g values of 2.218, 2.203, and 2.05 at 4.2 K. Similar g values were reported by Cho *et al.* (Figure 3.5).

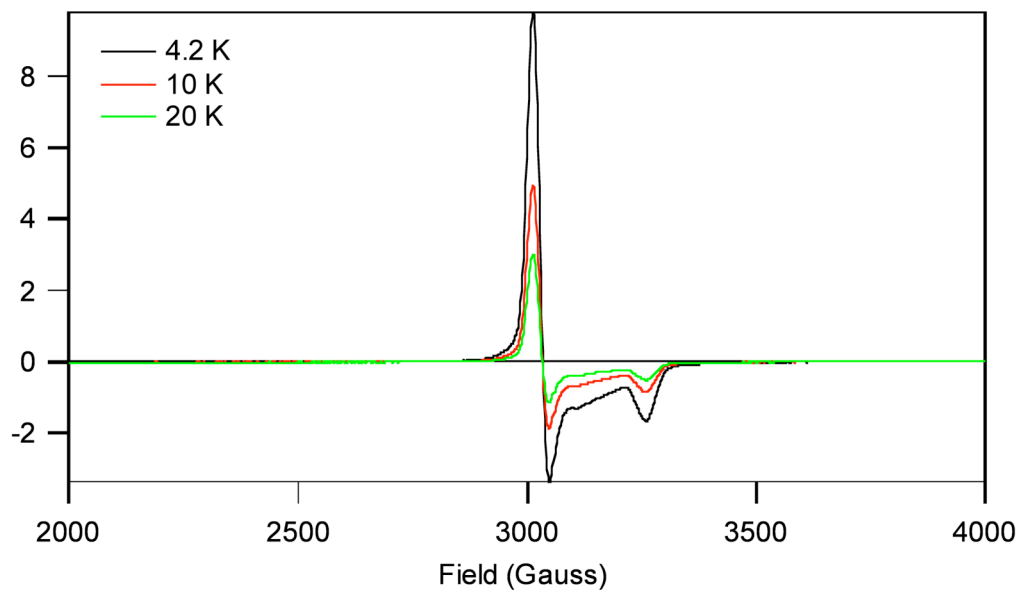


Figure 3.5 Electron paramagnetic resonance spectrum of $[\text{Ni}(\text{tmcyclen})(\text{O}_2)]\text{OTf}$ in THF, formed from reaction of $[\text{Ni}(\text{tmcyclen})(\text{CO})]\text{OTf}$ with O_2 . Parameters - frequency: 9.355 GHz, microwave power: 1.002 mW, attenuation: 23 dB, receiver gain: 49 dB, modulation amplitude: 2 G, modulation frequency: 100 kHz, time constant and conversion time: 163.84 ms.

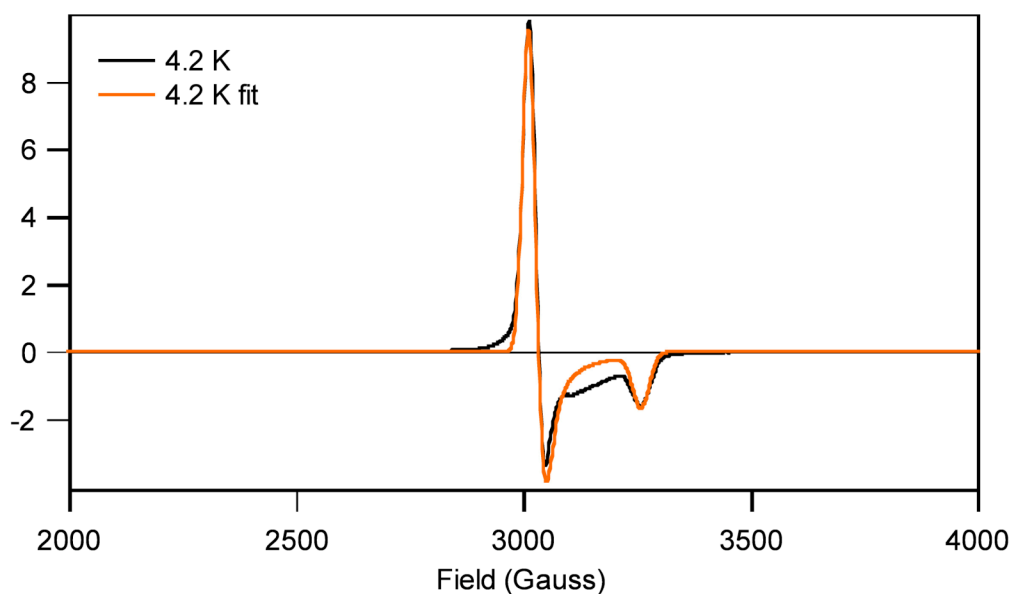


Figure 3.6 Electronic paramagnetic resonance spectrum of $[\text{Ni}(\text{tmcyclen})\text{O}_2]\text{OTf}$ in THF at 4.2 K and the fit of that data by WEPR program.

The above data demonstrate that when $[\text{Ni}(\text{tmcyclen})]\text{OTf}$ is oxygenated the Ni(III) “side-on” peroxo complex is formed. There was no indication of intermediates when using different oxygenation sources. The data show the smaller macrocycle is capable of stabilizing a higher oxidation state allowing for the formation of a Ni(III) peroxo complex. In addition, the flexibility of the macrocycle allows for a six coordinate species opposed to an “end-on” complex observed with the slightly larger macrocycle, TMC.

3.3 Reactivity of [Ni(tmcylen)(O₂)]OTf

3.3.1 Reactivity Studies Protocol

The reactivity of [Ni(tmcylen)(O₂)]OTf and [Ni(TMC)(O₂)]OTf was investigated using a variety of substrates. All experiments were completed under an inert atmosphere. In a typical experiment, the Ni(O₂) complex was formed first and a solution of the substrate was added under positive nitrogen pressure. The reaction was stirred for approximately 12 hours before being quenched with water and the organic product extracted with pentane or chloroform. The organic solution was dried over Na₂SO₄ and filtered. The products were identified and analyzed by GC and NMR spectroscopies. Authentic compounds were run by GC with dodecane as an internal standard to quantify product formation.

3.3.2 Reaction of [Ni(tmcylen)(O₂)]OTf with Phosphines, Sulfides, Olefins, and Activated C-H Bonds

Kieber-Emmons *et al.* reported that [Ni(TMC)(O₂)]OTf quantitatively oxidizes PPh₃ but does not oxidize less reactive substrates including sulfides and olefins.^[30] These experiments were repeated with the above protocol using PPh₃, styrene, thioanisole, dihydroanthracene, and 1,4-cyclohexene. These experiments were also conducted using nickel complexes prepared from O₂ or H₂O₂ sources. Quantitative

formation of OPPh_3 was observed in all cases; however, no reaction was noted for any of the remaining substrates.

The same studies were completed with $[\text{Ni}(\text{tmcyclen})(\text{O}_2)]^+$ prepared from both Ni(II) and Ni(I) starting materials. As with $[\text{Ni}(\text{TMC})(\text{O}_2)]^+$, no reactivity was observed with styrene, thioanisole, dihydroanthracene, and 1,4-cyclohexadiene. Interestingly, no oxidation of PPh_3 was detected.^[50] This shows a fundamental difference between $[\text{Ni}(\text{TMC})(\text{O}_2)]^+$ and $[\text{Ni}(\text{tmcyclen})(\text{O}_2)]^+$, where $[\text{Ni}(\text{TMC})(\text{O}_2)]^+$ has more nucleophilic character than $[\text{Ni}(\text{tmcyclen})(\text{O}_2)]^+$. Deformylation of aldehydes was identified by Cho *et al.* demonstrating the electrophilic character of $[\text{Ni}(\text{tmcyclen})(\text{O}_2)]^+$.^[50]

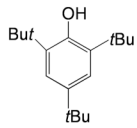
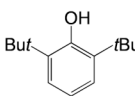
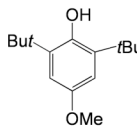
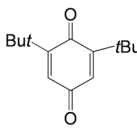
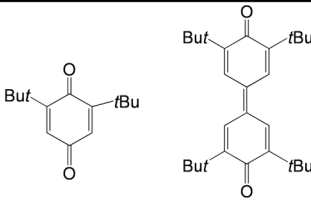
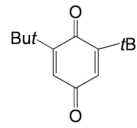
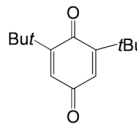
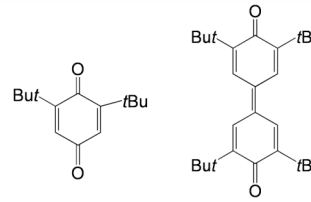
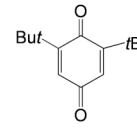
3.3.3 Reaction of $[\text{Ni}(\text{tmcyclen})(\text{O}_2)]\text{OTf}$ with Substituted Phenols

Reactions with substituted phenols were investigated with both $[\text{Ni}(\text{TMC})(\text{O}_2)]^+$ and $[\text{Ni}(\text{tmcyclen})(\text{O}_2)]^+$ to determine if these Ni complexes could oxidize these substrates. Recently, Maiti *et al.* reported a Cu(II)-superoxo complex, $[\text{Cu}(\text{TMG}_3\text{tren})(\eta^1\text{-O}_2)]^+$, which can effect hydrogen atom abstraction and subsequent oxidation or oxygenation of substituted phenols.^[51] Maiti and coworkers identified 2,6-*t*Bu₂-benzoquinone formation upon reaction of the Cu(II)-superoxo complex with either 2,4,6-*t*Bu₃-phenol or 2,6-*t*Bu₂-phenol. Conversely, reaction of the Cu(II)-superoxo complex with 4-MeO-2,6-*t*Bu₂-phenol lead to the 4-MeO-2,6-*t*Bu₂-phenoxy

radical (37%) as well as 4-MeO-2-*t*Bu-6-hydroperoxy phenol and 2,6-*t*Bu₂-benzoquinone (22%).^[51]

The substrates 2,6-*t*Bu₂-phenol, 2,4,6-*t*Bu₃-phenol, and 4-MeO-2,6-*t*Bu₂-phenol were reacted with [Ni(TMC)(O₂)]⁺ or [Ni(tmcyclen)(O₂)]⁺. In a typical experiment the Ni complex was brought up in CH₃CN and reacted with five equivalents of H₂O₂ and five equivalents of Et₃N to form the Ni-O₂ adduct. Under a positive pressure of N₂ a stoichiometric amount of phenol was added in a CHCl₃ solution. The reaction was stirred under N₂ at room temperature for 12 hours before being quenched by the addition of water. The phenol-derived products were extracted with pentane. The products and yields are summarized in Table 3.1. Using either Ni complex a stable phenoxy radical was not identified, though the products are similar to those observed by Maiti and coworkers. In addition, no aryl hydroperoxide was identified. Independent synthesis verified the identification of 2,2'',6,6''-*t*Bu₂-bisquinone. Control experiments run in the absence of metal complex confirmed the requirement of the metal complex in the oxidation reactions. The experiments were repeated for the both Ni complexes derived from dioxygen with very similar results, albeit in slightly lower yields. This could possibly be due to salt being carried through with the metal complex causing experiments to be run with a slight excess of phenol. The reactivity observed with both Ni complexes indicates [Ni(TMC)(O₂)]⁺ and [Ni(tmcyclen)(O₂)]⁺ complexes are capable of oxidizing phenols, perhaps via a hydrogen atom abstraction pathway, similar to the reaction promoted by other metal-superoxo complexes.

Table 3.1 Products and yields for substituted phenol reactivity studies.

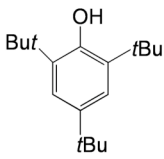
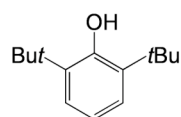
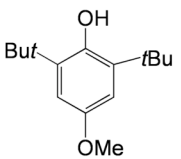
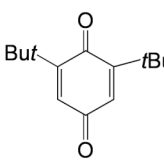
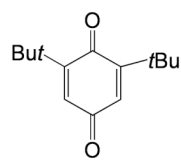
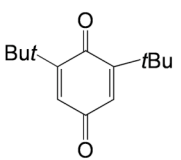
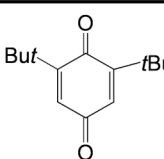
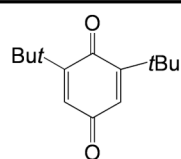
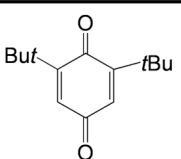
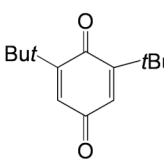
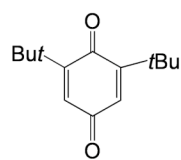
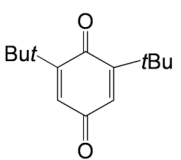
	 2,4,6-<i>t</i>Bu₃-phenol	 2,6-<i>t</i>Bu₂-phenol	 4-MeOH-2,6-<i>t</i>Bu₂-phenol
[Ni(tmcylen)(O₂)]⁺	 60% 2,6-<i>t</i>Bu₂-quinone	 10% 15% 2,6-<i>t</i>Bu₂-quinone 2,2',6,6'-<i>t</i>Bu₂-bisquinone	 80% 2,6-<i>t</i>Bu₂-quinone
[Ni(TMC)(O₂)]⁺	 15% 2,6-<i>t</i>Bu₂-quinone	 15% 20% 2,6-<i>t</i>Bu₂-quinone 2,2',6,6'-<i>t</i>Bu₂-bisquinone	 50% 2,6-<i>t</i>Bu₂-quinone

3.3.4 Reactivity studies when PhIO is used as an oxygen atom donor

The limited differences in reactivity between [Ni(TMC)(O₂)]⁺ and [Ni(tmcylen)O₂]⁺ may be due to a common intermediate that is responsible for the observed reactivity. PhIO reacts with metal salts to generate high valent metal-oxo complexes.^[52, 53, 54] In order to investigate the possibility of an oxo-nickel intermediate, PhIO was used as an oxo-transfer reagent. Subsequent reactivity with substituted phenols was explored. In a typical experiment, a stoichiometric amount of PhIO was added as a solid to a CHCl₃ solution containing the nickel(II) complex,

either $[\text{Ni}(\text{TMC})(\text{O}_2)]^+$ or $[\text{Ni}(\text{tmcyclen})\text{O}_2]^+$, followed by addition of the substituted phenol. The solution was stirred for 12 hours followed by a water quench. Organic products were extracted with pentane. Again, control experiments were completed, in which reactions with phenols were repeated with PhIO in the absence of nickel complex. Similar products were observed as to those detected when H_2O_2 or O_2 were used. Therefore, the reactivity observed proved to not be metal-mediated. The yields of the products indicate that PhIO is capable of oxidizing the phenols without the nickel salt.

Table 3.2 Products and yields for reactivity studies utilizing PhIO as an oxo-transfer agent

	 2,4,6- <i>t</i> Bu ₃ -phenol	 2,6- <i>t</i> Bu ₂ -phenol	 4-MeOH-2,6- <i>t</i> Bu ₂ -phenol
[Ni(tmcylen)]²⁺ + PhIO	 20% 2,6- <i>t</i> Bu ₂ -quinone	 15% 2,6- <i>t</i> Bu ₂ -quinone	 45% 2,6- <i>t</i> Bu ₂ -quinone
[Ni(TMC)]²⁺ + PhIO	 5% 2,6- <i>t</i> Bu ₂ -quinone	 15% 2,6- <i>t</i> Bu ₂ -quinone	 25% 2,6- <i>t</i> Bu ₂ -quinone
PhIO	 5% 2,6- <i>t</i> Bu ₂ -quinone	 5% 2,6- <i>t</i> Bu ₂ -quinone	 10% 2,6- <i>t</i> Bu ₂ -quinone

3.4 Oxygen transfer by [Ni(tmcylen)(O₂)]⁺ and [Ni(TMC)(O₂)]⁺

Cho *et. al.* demonstrated that [Ni(tmcylen)O₂]⁺ was capable of transferring the dioxygen ligand completely to another metal complex, [Mn(TMC)]²⁺, yielding [Mn(TMC)O₂]⁺, the first such transfer reported.^[50] The ability to transfer a dioxygen

ligand to other metal complexes, specifically Ni complexes, was investigated using $[\text{PhTt}^{\text{tBu}}]\text{Ni}(\text{CO})$ as the substrate. A THF solution of $[\text{Ni}(\text{tmcyclen})(\text{CO})]^+$ was oxygenated at room temperature with spectroscopic monitoring to ensure complete oxygenation. Excess oxygen was removed by repeated freeze/pump/thaw cycles. Addition of one equivalent of $[\text{PhTt}^{\text{tBu}}]\text{Ni}(\text{CO})$ in THF at low temperature resulted in a color change to purple. Though no intermediates were detected optically, features attributed to the formation of the bis(μ -oxo) dinickel(III) complex were observed, specifically transitions at 410 and 565 nm (Figure 3.6). It is proposed that complete oxygen transfer from the $[\text{Ni}(\text{tmcyclen})(\text{O}_2)]^+$ to the $[\text{PhTt}^{\text{tBu}}]\text{Ni}(\text{CO})$ occurs. Control experiments were conducted to ensure complete dioxygen removal prior to the introduction of the $[\text{PhTt}^{\text{tBu}}]\text{Ni}(\text{CO})$ complex. Similar results were observed with the $[\text{Ni}(\text{TMC})(\text{O}_2)]^+$ complex (Figure 3.7). The overall rate of formation for the bis(μ -oxo) dinickel(III) complex was different for $[\text{Ni}(\text{TMC})(\text{O}_2)]^+$ than that observed for $[\text{Ni}(\text{tmcyclen})(\text{O}_2)]^+$. Qualitatively, the transfer observed for $[\text{Ni}(\text{TMC})(\text{O}_2)]^+$ appears to be faster than $[\text{Ni}(\text{tmcyclen})(\text{O}_2)]^+$. However, further investigation is needed in order to determine the basis for this difference as well as to deduce general kinetic parameters.

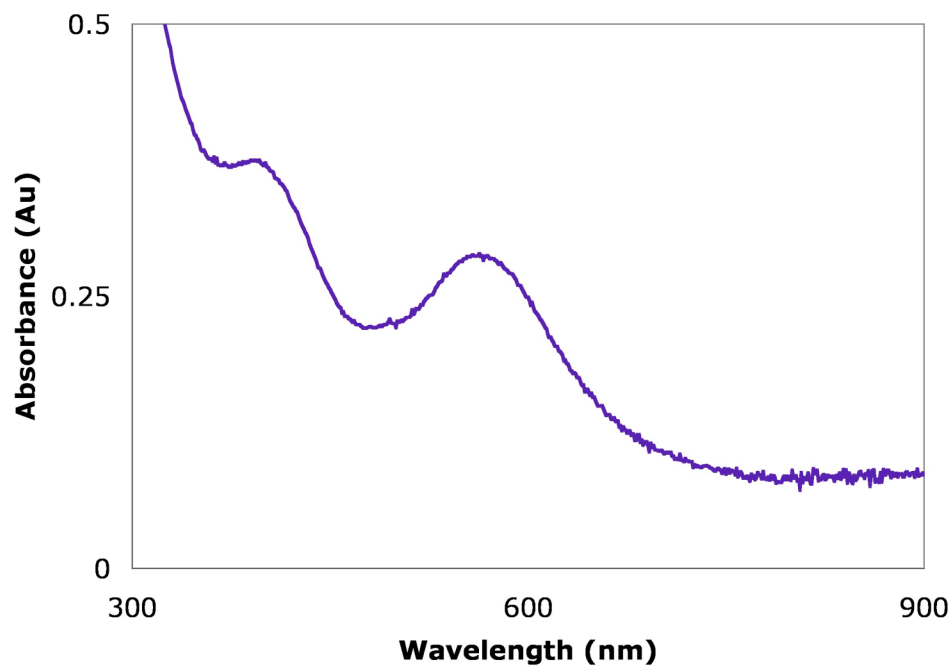


Figure 3.7 Optical spectrum for reaction of $[\text{Ni}(\text{tmcyclen})(\text{O}_2)]\text{OTf}$ with $(\text{PhTt}^{t\text{Bu}})\text{Ni}(\text{CO})$ in THF at -78°C . Features, $\lambda_{\text{max}} = 410$ and 565 nm, are in accord with formation of $[(\text{PhTt}^{t\text{Bu}})\text{Ni}]_2(\mu\text{-O})_2$.

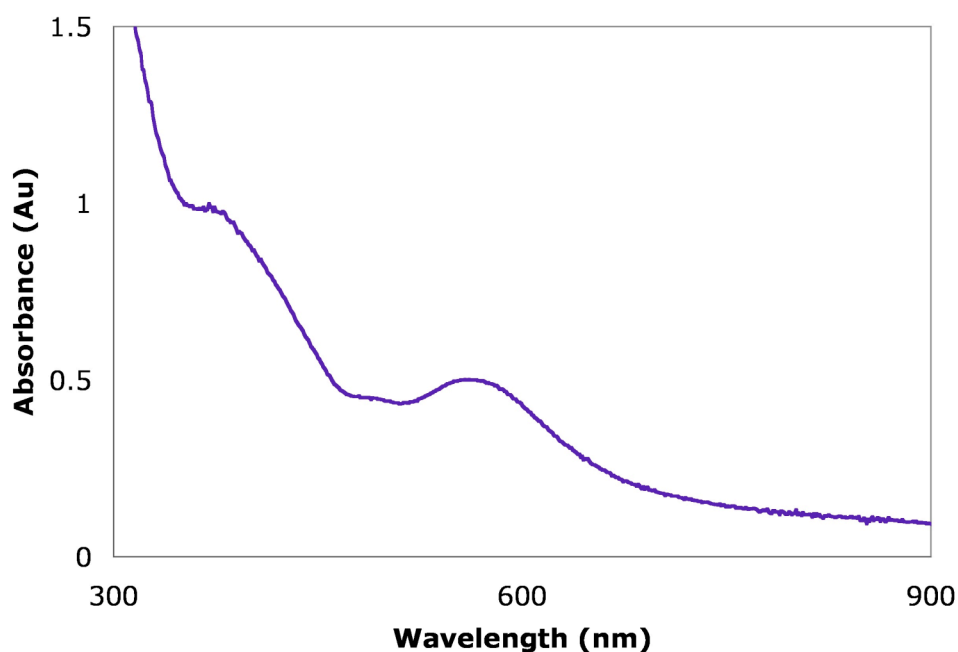


Figure 3.8 Optical spectrum for reaction of $[\text{Ni}(\text{TMC})(\text{O}_2)]\text{OTf}$ with $(\text{PhTt}^{t\text{Bu}})\text{Ni}(\text{CO})$ in THF at -78°C . Features, $\lambda_{\text{max}} = 410$ and 565 nm, are in accord with formation of $[(\text{PhTt}^{t\text{Bu}})\text{Ni}]_2(\mu\text{-O})_2$.

3.5 Conclusions

Understanding structure-function relationships is key not only in chemistry but in biology as well. Small molecules allow for the study of structure types that, to date, have yet to been identified in biology. Understanding of their electronic and spectroscopic properties allows for expansion of a library of knowledge. Herein, ligands were designed and synthesized with specific aims to expand the types of nickel-oxygen complexes that can be prepared from nickel(I)

precursors and O₂ and the effect of oxygenating nickel complexes via different routes. The smaller cavity and the flexibility of the tmcyclen macrocycle allowed for the formation of a “side-on” nickel(III)-peroxo complex. The reactivity of the complex indicated nucleophilic character, whereas the [Ni(TMC)(O₂)]⁺ complex had substantial electrophilic character. This work demonstrates how small changes in structure can drastically affect both the geometric and electronic properties of the nickel-oxygen complex formed, and thus the reactivity of the complex.

REFERENCES

1. Kasting, J. F. "Earth's early atmosphere" *Science* **1993**, 259, 920-26.
2. Sessions, A. L.; Doughty, D. M.; Welander, P. A.; Summons, R. E.; Newman, D. K. "The continue puzzle of the great oxidation event" *Current Biology* **2009**, 19, R567-74.
3. Liang, H.; Dahan, M.; Karlin, K. D. "Dioxygen-activating bio-inorganic model complexes" *Current Opinion in Chemical Biology* **1999**, 3, 168-75.
4. Hlavica, P. "Models and mechanisms of O-O bond activation by cytochromeP450 A critical assessment of the potential role of multiple active intermediates in oxidative catalysis" *Eur. J. Biochem.* **2004**, 271, 4335-4360.
5. Koltz, I. M.; Koltz, T. A. "Oxygen-carrying proteins: a comparison of the oxygenation reaction in hemocyanin and hemerythrin with that of hemoglobin" *Science.* **1955**, 121, 477-80.
6. Klinman, J. P. "The copper-enzyme family of dopamine β -monooxygenase and peptidylglycine α -hydroxylating monooxygenase: Resolving the chemical pathways for substrate hydroxylation" *J. of Biological Chemistry* **2006**, 281, 3013-16.
7. Ragsdale, S. W. "Nickel Biochemistry" *Current Opinion in Chemical Biology* **1998**, 2, 208-215.
8. Mulrooney, S. B.; Hausinger, R. P. "Nickel uptake and utilization by microorganisms" *FEMS Microbiology Reviews* **2003**, 27, 239-261.
9. Dai, Y.; Wensink, P. C.; Abeles, R. H. "One Protein, Two Enzymes" *J. Biol.Chem.* **1999**, 274, 1193-1195.
10. Kieber-Emmons, M. T. "Oxygen and sulfur activation by monovalent nickel". Ph.D. Dissertation, University of Delaware, 2008.
11. Ju, T.; Goldsmith, R.; Chai, S.; Maroney, M.; Pochapsky, S.; Pochapsky, T. "One Protein, Two Enzymes Revisited: A Structural Entropy Switch Interconverts the Two Isoforms of Acireductone Dioxygenase" *Journal of Molecular Biology* **2006**, 363, 823-834.

12. Al-Mjeni, F.; Ju, T.; Pochapsky, T. C.; Maroney, M. J. "XAS investigation of the structure and function of Ni in acireductone dioxygenase" *Biochemistry* **2002**, *41*, 6761-69.
13. Youn, H.-D.; Kim, E.-J.; Roe, J.-H.; Hah, Y. C.; Kang, S.-O. "A novel nickel-containing superoxide dismutase from *Streptomyces* spp." *Biochem. J.* **1996**, *318*, 889-896.
14. Barondeau, D. P.; Kassmann, C. J.; Bruns, C. K.; Tainer, J. A.; Getzoff, E. D. "Nickel Superoxide Dismutase Structure and Mechanism" *Biochemistry* **2004**, *43*, 8038-8047.
15. Carrington, P. E.; Al-Mjeni, F.; Zoroddu, M. A.; Costa, M.; Maroney, M. J. "Use of XAS for the elucidation of metal structure and function: applications to nickel biochemistry, molecular toxicology, and carcinogenesis" *Environ. Health Perspect* **2002**, *110 Suppl 5*, 705-8.
16. Choudhury, S. B.; Lee, J. W.; Davidson, G.; Yim, Y. I.; Bose, K.; Sharma, M. L.; Kang, S. O.; Cabelli, D. E.; Maroney, M. J. "Examination of the nickel site structure and reaction mechanism in *Streptomyces seoulensis* superoxide dismutase" *Biochemistry* **1999**, *38*, 3744-52.
17. Wuerges, J.; Lee, J.; Yim, Y.; Yim, H.; Kang, S.; carugo, K. D. "Crystal structure of nickel-containing superoxide dismutase reveals another type of active site" *Proc. Natl. Acad. Sci. U. S. A.* **2004**, *101*, 8569-74.
18. Pelmeshnikov, V.; Siegbahn, P. E. M. "Nickel superoxide dismutase reaction mechanism studied by hybrid density functional methods" *J. Am. Chem. Soc.* **2006**, *128*, 7466-75.
19. Prabhakar, R.; Morokuma, K.; Musaev, D. G. "A DFT study of the mechanism of Ni superoxide dismutase (NiSOD): role of the active site cysteine-6 residue in the oxidative half-reaction" *Journal of Computational Chemistry* **2006**, *27*, 1438-45.
20. Szilagyi, R. K.; Bryngelson, P. A.; Maroney, M. J.; Hedman, B.; Hodgson, K. O.; Solomon, E. I. "S K-edge x-ray absorption spectroscopic investigation of the Ni-containing superoxide dismutase active site: New structural insight into the mechanism" *J. Am. Chem. Soc.* **2004**, *126*, 3018-19.

21. Kieber-Emmons, M. T.; Riordan, C. G. "Dioxygen activation at monovalent nickel" *Acc. Chem. Res.* **2007**, *40*, 618-25.
22. Hikichi, S.; Yoshizawa, M.; Sasakura, Y.; Akita, M.; Moro-oka, Y. "First Synthesis and Structural Characterization of Dinuclear M(III) Bis(μ -oxo) Complexes of Nickel and Cobalt with Hydrotris(pyrazolyl)borate Ligand" *J. Am. Chem. Soc.* **1998**, *120*, 10567-10568.
23. Cho, J.; Furutachi, H.; Fujinami, S.; Tosha, T.; Ohtsu, H.; Ikeda, O.; Suzuki, A.; Nomura, M.; Uruga, T.; Tanida, H.; Kawai, T.; Tanaka, K.; Kitagawa, T. and Suzuki, M. "Sequential reaction intermediates in aliphatic C-H bond functionalization initiated by a bis(μ -oxo)dinickel(III) complex" *Inorg. Chem.* **2006**, *45*, 2873-85.
24. Mandimutsira, B. S.; Yamarik, J. L.; Brunold, T. C.; Gu, W.; Cramer, S. P.; Riordan, C. G. "Dioxygen Activation by a Nickel Thioether Complex: Characterization of a $\text{Ni}^{\text{III}}_2(\mu\text{-O})_2$ Core" *J. Am. Chem. Soc.* **2001**, *123*, 9194-9195.
25. Fujita, K.; Schenker, R.; Gu, W.; Brunold, T. C.; Cramer, S. P.; Riordan, C. G. "A Monomeric Nickel-Dioxygen Adduct Derived from a Nickel(I) Complex and O_2 " *Inorg. Chem.* **2004**, *43*, 3342-3326.
26. Bag, B.; Mondal, N.; Rosair, G.; Mitra, S. "The first thermally-stable singly oxo-bridged dinuclear Ni(III) complex" *Chem. Commun.* **2000**, 1729-30.
27. Brown, E. J.; Duhme-Klair, A. K.; Elliott, M. I.; Thomas-Oates, J. E.; Timmins, P. L.; Walkton, P. H. "The first μ_6 -peroxide transition-metal complex: $[\text{Ni}_8(\text{L})_{12}(\text{O}_2)]^{2+}$ " *Angew. Chem. Int. Ed.* **2005**, *44*, 1392-95.
28. Otsuka, S.; Nakamura, A.; Tatsuno, Y. "Oxygen Complexes of Nickel and Palladium. Formation, Structure, and Reactivities" *J. Am. Chem. Soc.* **1969**, *91*, 6994-6999.
29. Yao, S.; Bill, E.; Carsten, M.; Wieghardt, K.; Driess, M. "A "side-on" superoxonickel complex $[\text{LNi}(\text{O}_2)]$ with a square-planar tetracoordinate nickel(II) center and its conversion into $[\text{LNi}(\mu\text{-OH})_2\text{NiL}]$ " *Angew. Chem. Int. Ed.* **2008**, *47*, 7110-15.
30. Kieber-Emmons, M. T.; Annaraj, J.; Seo, M. S.; Van Heuvelen, K. M.; Tosha, T.; Kitagawa, T.; Brunold, T. C.; Nam, W.; Riordan, C. G. "Identification of

- an "end-on"-superoxo adduct, $[\text{Ni}(\text{tmc})(\text{O}_2)]^{+}$ " *J. Am. Chem. Soc.* **2006**, *128*, 14230-31.
31. Kieber-Emmons, M. T.; Schenker, R.; Yap, G. P. A.; Brunold, T. C.; Riordan, C. G. "Spectroscopic elucidation of a peroxo $\text{Ni}_2(\mu\text{-O}_2)$ intermediate derived from a nickel(I) complex and dioxygen" *Angew. Chem. Int. Ed.* **2004**, *43*, 6716-18.
 32. Hikichi, S.; Yoshizawa, M.; Sasakura, Y.; Komatsuzaki, H.; Moro-oka, Y.; Akita, M. "Structural Characterization and Intramolecular Aliphatic C-H Oxidation Ability of $\text{M}^{\text{III}}(\mu\text{-O})_2\text{M}^{\text{III}}$ Complexes of Ni and Co with the Hydrotris-(3,5-dialkyl-4-X-pyrazolyl)borate Ligands Tp^{Me_2} , X (X = Me, H, Br) and Tp^{iPr_2} " *Chem. Eur. J.* **2001**, *7*, 5011-5028.
 33. Kinneary, J. F.; Albert, J. S.; Burrows, C. J. "Mechanistic Studies of Alkene Epoxidation Catalyzed by Nickel(II) Cyclam Complexes. ^{18}O Labeling and Substituent Effects" *J. Am. Chem. Soc.* **1988**, *110*, 6124-6129.
 34. Kimura, E.; Machida, R. "A Mono-oxygenase Model for Selective Aromatic Hydroxylation with Nickel(II)-Macrocyclic Polyamines" *J. Chem. Soc., Chem. Commun.* **1984**, 499-500.
 35. Chen, D.; Martell, A. E. "Oxygen Insertion in the Ni(II) Complexes of Dioxopentaaza Macrocyclic Ligands" *J. Am. Chem. Soc.* **1990**, *112*, 9411-9412.
 36. Otsuka, S.; Nakamura, A.; Tatsuno, Y.; Miki, M. "Reactions of Dioxygen Complexes of Nickel and Palladium" *J. Am. Chem. Soc.* **1972**, *94*, 3761-3767.
 37. Schebler, P. J.; Mandimutsira, B. S.; Riordan, C. G.; Liable-Sands, L. M.; Incarvito, C. D.; Rheingold, A. L. "Organometallic cobalt(II) and nickel(II) complexes supported by thioether ligation: unexpected nickel alkylation by the borato ligand phenyl((*tert*-butylthio)methyl)borate" *J. Am. Chem. Soc.* **2001**, *123*, 331-32.
 38. Ge, P.; Riordan, C. G.; Yap, G. P. A.; Rheingold, A. L. "A Homoleptic Thioether Coordination Sphere That Supports Nickel(I)" *Inorg. Chem.* **1996**, *35*, 5408-5409.

39. Schenker, R.; Mandimutsira, B. S.; Riordan, C. G.; Brunold, T. C. "Spectroscopic and Computational Studies on $[(\text{PhTt}^{\text{tBu}})_2\text{Ni}_2(\mu\text{-O})_2]$: Nature of the Bis- μ -oxo (Ni^{3+})₂ "Diamond" Core" *J. Am. Chem. Soc.* **2002**, *124*, 13842-13855.
40. Fujita, K.; Rheingold, A. L.; Riordan, C. G. "Thioether-ligated nickel(I) complexes for the activation of dioxygen" *Dalton Trans.* **2003**, 2004-2005.
41. Schenker, R.; Kieber-Emmons, M. T.; Riordan, C. G.; Brunold, T. C. "Spectroscopic and computational studies on the trans- μ -1,2-peroxo-bridged dinickel species $[\{\text{Ni}(\text{tmc})\}_2(\text{O}_2)](\text{OTf})_2$: Nature of an end-on peroxo-nickel(II) bonding and comparison with peroxo-copper(II) bonding" *Inorg. Chem.* **2005**, *44*, 1752-62.
42. Neese, F. "Electronic Structure and Spectroscopy of Novel Copper Chromophores in Biology". Ph.D. Dissertation, University of Konstanz, 1997.
43. Barefield, E. K.; Wagner, F. "Metal Complexes of 1,4,8,11-Tetramethyl-1,4,8,11-tetraazacyclotetradecane, N-Tetramethylcyclam" *Inorg. Chem.* **1973**, *12*, 2435-39.
44. Sibert, J. W.; Cory, A. H.; Cory, J. G. "Lipophilic derivatives of cyclam as new inhibitors of tumor cell growth" *Chem. Commun.* **2002**, 154-55.
45. Oberholzer, M. R.; Neuburger, M.; Zehnder, M.; Kaden, T. A. "Metal Complexes with Macrocyclic ligands Part XXXVIII Steric effects in the copper(II) and nickel(II) complexes with tetra-*N*-alkylated 1,4,8,11-tetraazacyclotetradecanes" *Helvetica Chimica Acta* **1995**, *78*, 505-13.
46. Coates, J. H.; Hadi, D. A.; Lincoln, S. F. "The preparation, characterization and solution chemistry of some nickel(II) and copper(II) complexes of 1,4,7,10-tetramethyl-1,4,7,10-tetraazacyclododecane" *Aust. J. Chem.* **1982**, *35*, 903-09.
47. Kalligeros, G. A.; Blinn, E. L. "Strained five- and six-coordinated macrocyclic nickel(II) complexes" *Inorg. Chem.* **1972**, *11*, 1145-48.
48. Szalda, D. J.; Fujita, E.; Sanzenbacher, R.; Paulus, H.; Elias, H. "Syntheses and properties of nickel(I) and nickel(II) complexes of a series of macrocyclic N₄ ligands: Crystal structures of C-RSSR-[Ni^IHTIM](ClO₄), C-RSSR-

- [Ni^{II}HTIM](ClO₄)₂, C-RRSS-[Ni^{II}HTIM](ClO₄)₂ and [Ni^{II}TIM](ClO₄)₂ (HTIM = 2,3,9,10-tetramethyl-1,4,8,11-tetraazacyclotetradecane, TIM = 2,3,9,10-tetramethyl-1,4,8,11-tetraazacyclotetradeca-1,3,8,10-tetraene)" *Inorg. Chem.* **1994**, *33*, 5855-63.
49. Mejeritskaia, E.; Luo, F.; Kelly, C. A.; Koch, B.; Gundlach, E. M.; Blinn, E. L. "The reduction of carbon dioxide employing 1,4,7,10-tetramethyl-1,4,7,10-tetraazacyclododecane nickel(II) as a electron relay catalyst" *Inorganica Chimica Acta* **1996**, *246*, 295-99.
 50. Cho, J.; Sarangi, R.; Annaraj, J.; Kim, S. Y.; Kubo, M.; Ogura, T.; Solomon, E. I.; Nam, W. "Geometric and electronic structure and reactivity of a mononuclear "side-on" nickel(III)-peroxo complex" *Nature Chemistry* **2009**, *1*, 568-72.
 51. Maiti, D.; Lee, D. H.; Gaoutchenova, K.; Würtele, C.; Holthausen, M. C.; Narducci Sarjeant, A. A.; Sundermeyer, J.; Schindler, S.; Karlin, K. D. "Reactions of a copper(II) superoxo complex lead to C-H and O-H substrate oxygenation: Modeling copper-monooxygenase C-H hydroxylation" *Angew. Chem. Int. Ed.* **2008**, *47*, 82-85.
 52. Que, L. "The road to non-heme oxoferryls and beyond" *Acc. Chem. Res.* **2007**, *40*, 493-500.
 53. Song, W. J.; Sea, M. S.; George, S. D.; Ohta, T.; Song, R.; Kang, M. K. Tosha, T.; Kitagawa, T.; Solomon, E. I.; Nam, W. "Synthesis, Characterization, and reactivates of manganese(V)-oxo porphyrin complexes" *J. Am. Chem. Soc.* **2007**, *129*, 1268-77.
 54. Qin, K.; Incarvito, C. D.; Rheingold, A. L.; Theopold, K. H. "Hydrogen atom abstraction by chromium(IV) oxo complex derived from O₂" *J. Am. Chem. Soc.* **2002**, *124*, 14008-14009.

APPENDIX A
CRYSTALLOGRAPHIC DATA

Compound	Tetrapivaloyl cyclam	Tetraneopentyl cyclam
Identification Code	Char 205	Char 209a
Empirical Formula	C30 H64 N4	C30 H56 N4 O4
Formula Weight	480.85	536.79
Color, Habit	Colorless, Needles	Colorless, Needles
Crystal System	Tetragonal	Monoclinic
Space Group	P4(2)/n	P2(1)/c
<i>a</i> , Å	22.853(2)	13.313(4)
<i>b</i> , Å	22.853(2)	11.511(3)
<i>c</i> , Å	6.0964(11)	11.770(3)
α , deg	90	90
β , deg	90	115.158(4)
γ , deg	90	90
<i>V</i> , Å ³	3183.8(7)	1632.6(8)
<i>Z</i>	4	2
Temperature (K)	120	120
<i>D</i> _{calcd} , g/cm ³	1.003	1.092
θ range, deg	1.78-28.31	1.69-28.38
GOF (<i>F</i> ²)	1.029	1.037
μ (Mo, K α) mm ⁻¹	0.058	0.072
Reflections	31312	20992
Unique	3957	4074
<i>R</i> (int)	0.1108	0.0301
<i>R</i> 1	0.0576	0.0480
<i>wR</i> 2	0.1212	0.1324

Quantity Maximized = $R(wF^2) = \Sigma[w(F_o^2)^2]/\Sigma[wF_o^2]^{1/2}$; $R = \Sigma \Delta/\Sigma(F_o)$, $\Delta = |(F_o - F_c)|$, $w = 1/[\sigma^2(F_o^2) + (aP)^2 + bP]$, $P = [2F_c^2 + \text{Max}(F_o, 0)]/3$

Compound	(N ₂ C ₁₅ H ₂₉) ₂ CuCl ₄	[Ni(tmcyclen)CO](OTf)
Identification Code	Char 207a	Char 258
Empirical Formula	C ₃₀ H ₅₈ Cl ₄ Cu N ₄	C ₁₄ H ₂₈ F ₃ N ₄ Ni O ₄ S
Formula Weight	680.14	464.17
Color, Habit	Orange, Blocks	Green, Plates
Crystal System	Tetragonal	Monoclinic
Space Group	I4(1)/a	P2(1)/c
<i>a</i> , Å	11.718(2)	15.968(7)
<i>b</i> , Å	11.718(2)	16.662(7)
<i>c</i> , Å	26.378(10)	15.977(7)
α , deg	90	90
β , deg	90	101.854(7)
γ , deg	90	90
<i>V</i> , Å ³	3622.1(17)	4160(3)
<i>Z</i>	4	8
Temperature (K)	120	200
<i>D</i> _{calcd} , g/cm ³	1.247	1.482
θ range, deg	1.90-28.34	1.22-28.31
GOF (<i>F</i> ²)	1.089	1.019
μ (Mo, K α) mm ⁻¹	0.922	1.085
Reflections	24571	57000
Unique	2264	10495
<i>R</i> (int)	0.0237	0.0473
<i>R</i> 1	0.0297	0.0606
<i>wR</i> 2	0.0785	0.1584

Quantity Maximized = $R(wF^2) = \Sigma[w(F_o^2)^2]/\Sigma[wF_o^2]^{1/2}$; $R = \Sigma \Delta/\Sigma(F_o)$, $\Delta = |(F_o - F_c)|$, $w = 1/[\sigma^2(F_o^2) + (aP)^2 + bP]$, $P = [2F_c^2 + \text{Max}(F_o, 0)]/3$